

Nature's Machinery, Repurposed: Expanding the Repertoire of Iron-Dependent Oxygenases

Noah P. Dunham, and Frances H. Arnold

ACS Catal., Just Accepted Manuscript • DOI: 10.1021/acscatal.0c03606 • Publication Date (Web): 28 Sep 2020

Downloaded from pubs.acs.org on September 29, 2020

Just Accepted

"Just Accepted" manuscripts have been peer-reviewed and accepted for publication. They are posted online prior to technical editing, formatting for publication and author proofing. The American Chemical Society provides "Just Accepted" as a service to the research community to expedite the dissemination of scientific material as soon as possible after acceptance. "Just Accepted" manuscripts appear in full in PDF format accompanied by an HTML abstract. "Just Accepted" manuscripts have been fully peer reviewed, but should not be considered the official version of record. They are citable by the Digital Object Identifier (DOI®). "Just Accepted" is an optional service offered to authors. Therefore, the "Just Accepted" Web site may not include all articles that will be published in the journal. After a manuscript is technically edited and formatted, it will be removed from the "Just Accepted" Web site and published as an ASAP article. Note that technical editing may introduce minor changes to the manuscript text and/or graphics which could affect content, and all legal disclaimers and ethical guidelines that apply to the journal pertain. ACS cannot be held responsible for errors or consequences arising from the use of information contained in these "Just Accepted" manuscripts.

Nature's Machinery, Repurposed: Expanding the Repertoire of Iron-Dependent Oxygenases

Noah P. Dunham and Frances H. Arnold*

Division of Chemistry and Chemical Engineering, California Institute of Technology, 1200 East California Boulevard, MC 210-41, Pasadena, California 91125, United States

ABSTRACT: Iron is an especially important redox-active cofactor in biology because of its ability to mediate reactions with atmospheric O₂. Iron-dependent oxygenases exploit this earth-abundant transition metal for the insertion of oxygen atoms into organic compounds. Throughout the astounding diversity of transformations catalyzed by these enzymes, the protein framework directs reactive intermediates toward the precise formation of products, which, in many cases, necessitates the cleavage of strong C–H bonds. In recent years, members of several iron-dependent oxygenase families have been engineered for new-to-nature transformations that offer advantages over conventional synthetic methods. In this Perspective, we first explore what is known about the reactivity of heme-dependent cytochrome P450 oxygenases and nonheme iron-dependent oxygenases bearing the 2-His-1-carboxylate facial triad by reviewing mechanistic studies with an emphasis on how the protein scaffold maximizes the catalytic potential of the iron-heme and iron cofactors. We then review how these cofactors have been repurposed for abiological transformations by engineering the protein frameworks of these enzymes. Finally, we discuss contemporary challenges associated with engineering these platforms and comment on their roles in biocatalysis moving forward.

KEYWORDS: *biocatalysis, enzymology, directed evolution, mechanism, oxygenase, cytochrome P450*

1. INTRODUCTION

Nature's finest catalytic machinery is comprised of protein-based enzymes. Constructed mainly of polypeptide chains of the twenty genetically encoded amino acids, enzymes can assume a multiplicity of three-dimensional forms, which is the foundation for the remarkable diversity of chemical transformations that are catalyzed with the efficiency and selectivity required to support a living organism.¹ While a great deal of this catalysis can be achieved within the manifold of functional groups provided by the canonical proteinogenic amino acids, whether by simple acid-base reactions or through intermediary covalent linkages, many essential biochemical transformations necessitate catalytic capabilities that exceed what is offered by these residues. The solution comes in the form of metallic or organic cofactors, with which many proteins are equipped to expand their catalytic repertoires. In this context, the interplay between the protein and cofactor is crucially important: the acquired catalytic function stemming from the unique properties of the cofactor is elicited or amplified by the protein environment. Cofactor-protein complexes achieve levels of activity and chemo-, regio-, and stereoselectivity that far surpass that which is produced by either component separately.

Since the emergence of our aerobic atmosphere, redox-active metals have taken on additional functions. Because the direct reaction of molecular oxygen (O_2) in its thermodynamically favored triplet ground state with singlet organic compounds is generally spin-forbidden, metallocofactors with unpaired *d*-electrons, such as iron, provide a channel to mediate such reactions by reductive activation of this atmospherically prevalent molecule.²⁻⁴ The resulting metal-oxygen species serve as intermediates in pathways that are central to biology, Complex IV of the electron transport chain in aerobic respiration perhaps being the most notable example. Many other metalloenzymes activate O_2 to insert oxygen atoms into the structures of their organic

1
2
3 substrates.⁵ These oxygenases have provided us with powerful catalysts for biosynthesis and
4
5 synthetic chemistry.
6

7
8 In this Perspective, we discuss the role of iron both in the heme complex and as free ferrous
9
10 ion, and how its catalytic potential is maximized by proteins to effect oxygenase reactions. Toward
11
12 this goal, we recount the catalytic cycles of heme-dependent cytochromes P450 and nonheme iron-
13
14 dependent oxygenases that utilize the 2-His-1-carboxylate facial triad, highlighting throughout
15
16 how the protein sequence imparts selective catalysis. The knowledge accumulated from decades
17
18 of rigorous mechanistic studies demonstrates the advantages of using an enzyme to achieve such
19
20 outcomes, especially in cases where direct comparison can be made to the reactivity of the protein-
21
22 free cofactor.
23
24
25

26 From this foundational understanding of how Nature's catalytic machinery controls
27
28 reactivity and specific product outcomes, we bring the discussion to contemporary challenges in
29
30 chemical synthesis by showing how the catalytic capabilities of natural enzymes can lead to
31
32 discovery and optimization of new-to-nature transformations. Leveraging enzymes for the
33
34 synthesis of high-value chemicals constitutes a powerful strategy with broad potential.⁶ While
35
36 natural evolution has sharpened the myriad native functions of enzymes for specific biological
37
38 advantages, it would be imprudent to look upon these functions as limits of achievability. Applying
39
40 directed evolution, it is now feasible, even uncomplicated, to enhance the latent activities of
41
42 enzymes for non-natural chemistry and further expand our synthetic toolbox,⁷ just as Nature has
43
44 expanded hers over millions of years. In other words, the well of innovation is just waiting to be
45
46 tapped. Recently, a number of iron-dependent oxygenases have been engineered to realize such a
47
48 goal. Herein, we summarize the efforts of several research groups to push the hemoprotein and
49
50
51
52
53
54
55
56
57
58
59
60

1
2
3 nonheme 2-His-1-carboxylate enzymatic platforms into the world of abiological catalysis, and then
4
5 speculate on the future impact on chemical synthesis.
6

7
8 Eliciting new reactivity from cofactor-dependent enzymes and honing this reactivity by
9
10 directed evolution is truly at the interface between enzymology and synthetic chemistry.
11
12 Inspiration drawn from both fields can contribute to transformational advancements in our ability
13
14 to craft molecules using biocatalysts. While the focus of this Perspective is narrowed to iron-
15
16 dependent oxygenases, our broader goal is to inspire researchers to examine existing biological
17
18 cofactors as potential sources of new and useful chemistry, from which fundamental knowledge
19
20 stands to be extracted and new synthetic tools stand to be developed.
21
22
23
24
25

26 **2. HEME**

27 **2.1. Structure and Reactivity**

28
29 Heme cofactors employ the organic porphyrin framework to coordinate iron for a diversity of
30
31 functions.⁸ The 18π electrons of the core structure (**Figure 1**, red substructure), which consists of
32
33 four pyrrole subunits connected by methine bridges, are thought to be the basis of the cofactor's
34
35 aromatic character,⁹ the key contributor to its absorption properties and the generation of π -cation
36
37 radicals during the formation of high-valent iron intermediates.¹⁰ The resulting planar structure
38
39 coordinates the iron in a tetradentate fashion and occupies an entire plane of the octahedron. One
40
41 or both coordination sites perpendicular to this equatorial plane can be occupied by additional axial
42
43 ligands (X in **Figure 1**), which often play a crucial role in tuning the electronic properties of the
44
45 metal (*vide infra*).¹¹ In the active site of an enzyme, these ligands are contributed by amino acid
46
47 side-chains.
48
49
50
51
52
53
54
55
56
57
58
59
60

Heme's impressive catalytic repertoire is evident throughout its assortment of biological functions. From oxygen maintenance^{12,13} and electron transfer¹⁴ to decomposition of harmful oxygen species^{15,16} and facilitating an array of chemically challenging oxidative transformations,¹⁷⁻²¹ Nature has given this special cofactor a starring role. Heme has also been an inspiration to chemists for decades. Their efforts have not only yielded model complexes that elevated our understanding of hemoproteins, but also afforded a collection of biomimetic catalysts that have addressed a number of synthetic challenges.

These synthetic porphyrins have been extensively reviewed elsewhere.^{19,22-26}

Although Nature and humanity together have leveled a great deal of attention on heme, the natural forms of the cofactor by itself have found very limited use in biology as well as industrial pursuits. Thus, the question must be asked: how does the hemoprotein environment tune the cofactor such that the desired reactivity is achieved? Here we strive to answer this question in the context of cytochromes P450, the family of hemoproteins that have been described as 'a biological blowtorch'.²⁷ These enzymes catalyze a suite of aliphatic and aromatic C-H oxidations,^{28,29} heteroatom oxidations,^{30,31} olefin epoxidations,³² C-C desaturations,^{33,34} and more,^{18,35} rendering them an ideal subject for a case study on how the polypeptide chain can activate and tune the heme cofactor for highly selective transformations that are not observed in the absence of the protein scaffold.

2.2. C-H Hydroxylation Catalyzed by Cytochromes P450

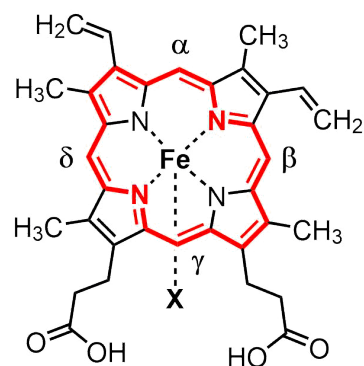
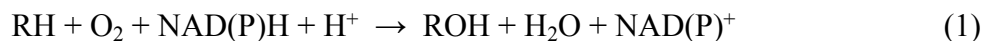


Figure 1. Structure of heme B. The bolded red bonds constitute the 18π electrons of the aromatic system in the [18]annulene model. X represents the axially coordinated protein ligand.

1
2
3 Cytochromes P450—named for the 450 nm absorption band observed with the reduced, CO-bound
4 state of the heme B cofactor³⁶—are found throughout every kingdom of life.³⁷ P450s coordinate
5 one of the two axial sites of the iron center with a cysteine ligand, leaving the other open for
6 binding of water or O₂. In the hydroxylation reaction, the net four-electron reduction of O₂ is
7 balanced by the two-electron oxidations of both NAD(P)H and the aliphatic C–H bond undergoing
8 oxygenation (**Equation 1**).¹⁸ Amazingly, the bond dissociation energies (BDE) of the targeted C–
9 H bonds can range as high as 102.9 kcal/mol,³⁸ an energy barrier that is overcome by reactive high-
10 valent iron-oxo intermediates. Throughout the step-by-step mechanism presented below, we
11 highlight the role of the protein scaffold and its contributing ligands in facilitating the formation
12 and directing the reactivity of these reactive intermediates.
13
14
15
16
17
18
19
20
21
22
23
24
25



26
27
28 In the resting state of the P450 active site, a water ligand occupies the sixth coordination
29 site of the low-spin ($S = 1/2$) Fe(III) cofactor (**Figure 2, state I**).^{11,18,39} Binding of the substrate
30 then displaces this axially coordinated water, which is important for two main reasons: (1) an axial
31 coordination site is now open for binding of O₂, and (2) the change in the coordination environment
32 shifts the iron to a high-spin ($S = 5/2$) state (state **II**).^{11,18} The latter consequence brings the redox
33 potential of the iron into the range of the corresponding cytochrome P450 reductase, which then
34 delivers an electron originating from NAD(P)H through the reduced form of its flavin
35 mononucleotide (FMN) cofactor.^{40–42} The coupling of this protein-controlled substrate binding
36 event with the reorganization of the ligand sphere effectively prevents entrance into the catalytic
37 cycle in the absence of substrate. It is worthy of note that while this substrate-induced spin-shift
38 strategy is a classic example of the control of electron flow in P450 catalysis, it is not universally
39 employed within the family. Alternative mechanisms have been reviewed elsewhere.⁴³
40
41
42
43
44
45
46
47
48
49
50
51
52
53
54
55
56
57
58
59
60

Reduction of the heme to Fe(II) triggers binding and reduction of O₂ to yield a ferric superoxo species (**Figure 2**, state IV), an intermediate that, if neglected, will produce harmful reactive oxygen species (ROS).⁴⁴ Thus, efficient delivery of a second electron and a proton are required at this stage to push the reaction forward toward the formation of the ferric hydroperoxo intermediate known as compound 0 (state VI).⁴⁵ This sequence, in addition to the initial reduction of the cofactor, necessitates precisely controlled access of the partner P450 reductase to the P450

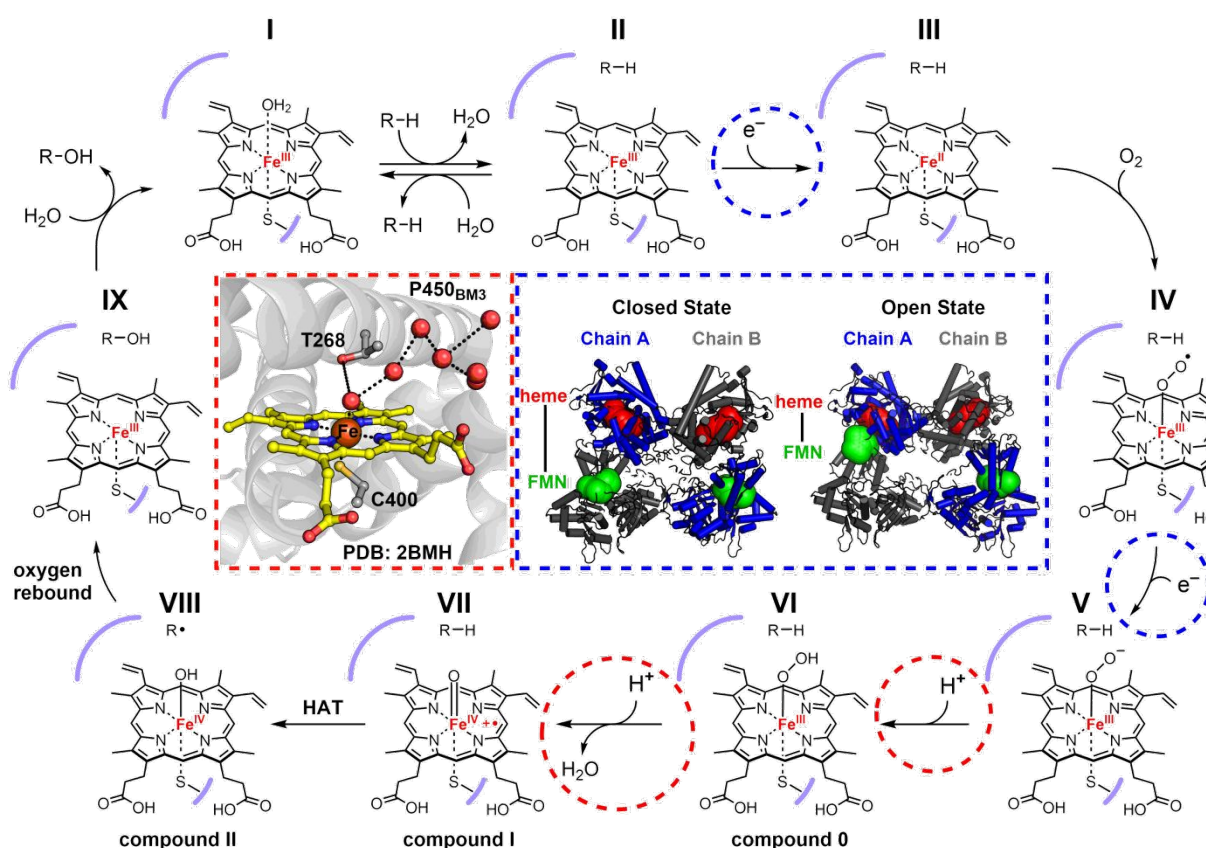


Figure 2. Mechanism of P450-catalyzed hydroxylation. The red inset (left) depicts the active site of the P450_{BM3} heme domain in the substrate-free crystal structure (PDB: 2BMH). The conserved T268 residue sits directly above the heme, in close contact with an ordered water network (red spheres) for the proton-transfer steps. The blue inset (right) shows the conformational shift between the closed and open states of the full-length P450_{BM3} dimeric complex (models derived from cryo-EM maps EMD: 20785 and EMD: 20786), which brings the heme (red spheres) from one monomer and FMN (green spheres) from the other in close proximity for the electron transfer steps.

1
2
3 active site. Complementing the years of rigorous explorations into this process,⁴⁶ the recently
4 solved single-particle cryo-EM structure of the full-length cytochrome P450 from *Bacillus*
5 *megaterium* (P450_{BM3}), a self-sufficient P450 with the partner reductase fused into a single
6 polypeptide chain, is an excellent model of how such control can be imparted by the protein
7 framework.⁴⁷ This structure provides a clear picture of how the dimeric complex can exist in open
8 and closed states, and how a conformational shift to the former brings the FMN cofactor of one
9 monomer into close proximity with the heme of the other, presenting a mechanism by which
10 electrons can be delivered to the cofactor in a manner controlled at the quaternary level of the
11 protein structure (blue inset). Meanwhile, a conserved threonine residue (T268 in P450_{BM3})
12 positioned above the heme likely facilitates the proton transfer either by direct interaction with
13 distal oxygen of the ferric peroxo intermediate (state **V**), or by extending its access to a nearby
14 water network (red inset).⁴⁸⁻⁵⁰

15
16
17
18
19
20
21
22
23
24
25
26
27
28
29
30
31 This conserved threonine residue also plays a crucial role in the subsequent O–O bond
32 scission step by assisting the delivery of a second proton to the distal oxygen of compound 0
33 (**Figure 2**, red inset), which results in release of water and formation of compound I (state **VII**).
34 Mutation of this threonine residue to alanine in either P450_{BM3} or P450_{CAM} diminished
35 hydroxylation activity and increased production of H₂O₂.^{48,49} The uncoupling of O₂ reduction from
36 substrate oxidation highlights the importance of precision proton delivery for efficient O–O bond
37 scission. Moreover, a recent study showed that a glutamic acid substitution allowed these P450s
38 to operate as peroxygenases, whereby substrate oxidation could be achieved through the peroxide
39 shunt pathway.⁵¹ These “pull” effects are complemented by the “push” effect exerted by the axial
40 cysteine ligand: the strong σ -donation from the thiolate, which effectively drives electron density
41 into the antibonding O–O orbital, also contributes to productive O–O bond heterolysis.^{11,19,52}

1
2
3 The two additional electrons required for reduction of hydrogen peroxide to water and O–
4 O bond scission are afforded by the iron and the organic porphyrin scaffold, resulting in the
5 formation of the high-valent Fe(IV)-oxo (ferryl) π -cation radical species known as compound I
6 (Figure 2, state VII).^{10,53} This potent oxidant intermediate facilitates hydrogen atom transfer
7 (HAT) from the substrate C–H bond to the cofactor, generating the Fe(IV)-hydroxide species
8 known as compound II and a substrate radical (state VIII).⁵⁴ The reaction cycle is completed by
9 transfer of the oxygen ligand to the carbon-centered radical (termed oxygen rebound, state VIII to
10 IX),⁵⁵ release of the hydroxylated product, and then rebinding of the water, returning the cofactor
11 to its resting state (state IX to I).¹⁸
12
13
14
15
16
17
18
19
20
21
22
23

24 During this sequence, P450s exhibit exquisite control over highly reactive intermediates
25 (e.g., compound I) to achieve productive cleavage of the substrate C–H bond while preventing the
26 oxidation of readily oxidizable amino acids within its own framework, such as tyrosines and
27 tryptophans. The axial cysteine ligand was initially posited to play a crucial role in the prevention
28 of such undesired reactions because it is present in all P450s and chloroperoxidase (CPO),¹¹ the
29 members of the hemoprotein family known to cleave strong C–H bonds. Green, Dawson, and Gray
30 postulated the difference in free energy between the productive C–H activation pathway and
31 nonproductive tyrosine oxidation pathway was largely dependent on the pK_a of the resulting
32 compound II, which was increased by the strong electron donation from the thiolate ligand.^{56,57} In
33 2013, Green and coworkers validated this hypothesis by trapping and characterizing compound II
34 of *Streptomyces coelicolor* CYP158 at differing pH values, determining its pK_a to be nearly 12
35 (more than 8 orders of magnitude more basic than the histidine-ligated heme peroxidases).^{54,56} This
36 change in axial ligand from histidine to cysteine alters the thermodynamic favorability of tyrosine
37 oxidation (via uncoupled proton and electron transfer) over substrate C–H bond cleavage (via
38
39
40
41
42
43
44
45
46
47
48
49
50
51
52
53
54
55
56
57
58
59
60

1
2
3 HAT) from ~14 kcal/mol to only 3 kcal/mol, bringing the P450-catalyzed C–H oxidation reaction
4 into the range of kinetic control.⁵⁴ These conclusions were further supported by the correlation of
5
6 a shorter Fe–S bond length with increased reactivity in P450s and CPOs,⁵⁸ and then later by the
7
8 increase in reactivity of a selenocysteine-ligated P450,⁵⁹ which exhibits even stronger electron
9
10 donation to the metal center than its sulfur counterpart. It is worthy of mention that other heme-
11
12 dependent oxygenases, such as tryptophan 2,3-dioxygenase and indoleamine 2,3-dioxygenase,
13
14 indeed utilize histidine axial ligands to direct high-valent iron intermediates, but activation of their
15
16 aromatic substrates presents a distinct set of challenges requiring divergent catalytic solutions. The
17
18 mechanisms of these transformations have been discussed elsewhere.^{60,61}
19
20
21
22
23

24 The decades of P450-centered research summarized above illustrate how the interplay
25
26 between peptide and cofactor can achieve reactivity that is nonexistent with either individual
27
28 component. The hydroxylation pathway is just one of many examples: Nature has tuned the P450
29
30 peptide-heme interaction for many other catalytic functions. From the perspective of the protein
31
32 engineer, a question that naturally follows is: can this remarkable catalytic machinery be hijacked
33
34 for abiological reactions and likewise tuned to achieve useful levels of activity and selectivity?
35
36
37
38
39

40 **2.3. New Hemoprotein Activities Emerge**

41 In recent years, our understanding of reactions catalyzed by hemoproteins and the characterization
42
43 of their reaction intermediates have been leveraged to develop new reactivities, which, combined
44
45 with engineering techniques such as directed evolution, have furnished a suite of powerful
46
47 hemoprotein catalysts. The examples recounted below are not intended to serve as a detailed
48
49 analysis of contributions to synthetic methodology, but rather to summarize that which is currently
50
51 possible with hemoprotein biocatalysts.
52
53
54
55
56
57
58
59
60

1
2
3 Inspired by the powerful transition metal-catalyzed carbene-transfer reactions developed
4 by synthetic chemists,⁶² Coelho, Brustad, and coworkers hypothesized that the heme cofactor
5 could form analogous metal-carbenoid intermediates, as they would have an isolobal relationship
6 with compound I.⁶³ The carbene could then be transferred, for example, to an olefin substrate to
7 form a cyclopropane product, similar to native P450-catalyzed epoxidation reactions. Indeed,
8 P450_{BM3} exhibited activity for the cyclopropanation of styrene with ethyl diazoacetate (EDA) as
9 the carbene precursor, which forms the iron-carbenoid intermediate upon loss of N₂.⁶⁴ Although
10 this reaction is also catalyzed by free hemin in the presence of dithionite, the protein environment
11 enforced a different selectivity of the product configuration. Screening a collection of P450
12 variants identified P450_{BM3}-CIS, which catalyzed the reaction with 199 total turnovers (TTNs), a
13 71:29 *cis/trans* ratio, and up to a 94% enantiomeric excess (% *ee*)—a significant improvement in
14 both activity and selectivity over the cofactor alone.
15
16
17
18
19
20
21
22
23
24
25
26
27
28
29
30

31 Coelho and Brustad then initiated a directed evolution campaign to generate even more
32 efficient catalysts, screening this new function in whole *Escherichia coli* cells. Their experiments
33 suggested that the cofactor was predominantly active in the Fe(II) state, as the reaction occurred
34 optimally in the presence of dithionite and the absence of O₂. Moreover, reduction of the cofactor
35 by the native NADPH-dependent reductase domain was unsuccessful, suggesting that the non-
36 native substrate fails to trigger the necessary shift in the iron's spin state, as observed in the native
37 reaction sequence (**Figure 2**). These roadblocks to enzyme-catalyzed cyclopropanation *in vivo*
38 were circumvented by mutating the axial cysteine ligand, which, as described above, plays a major
39 role in tuning the electronics of the cofactor.⁶⁵ Indeed, substitution with the less electron-donating
40 serine in P450_{BM3} (named P411_{BM3} for the Soret band shift from 450 nm to 411 nm) resulted in a
41 127 mV increase in the resting-state reduction potential ($E^{\circ} \text{Fe[III/II]} = -293 \text{ mV}$), bringing it into
42
43
44
45
46
47
48
49
50
51
52
53
54
55
56
57
58
59
60

the range of the reductase domain (E° NADP⁺/NADPH = -320 mV). Exchanging the axial cysteine for serine in P450_{BM3}-CIS (furnishing P411_{BM3}-CIS) abolished the competing epoxidation reaction, even in the presence of O₂. However, the P411 enzyme catalyzed the styrene cyclopropanation reaction with up to 67,800 TTN in whole cells.⁶⁵

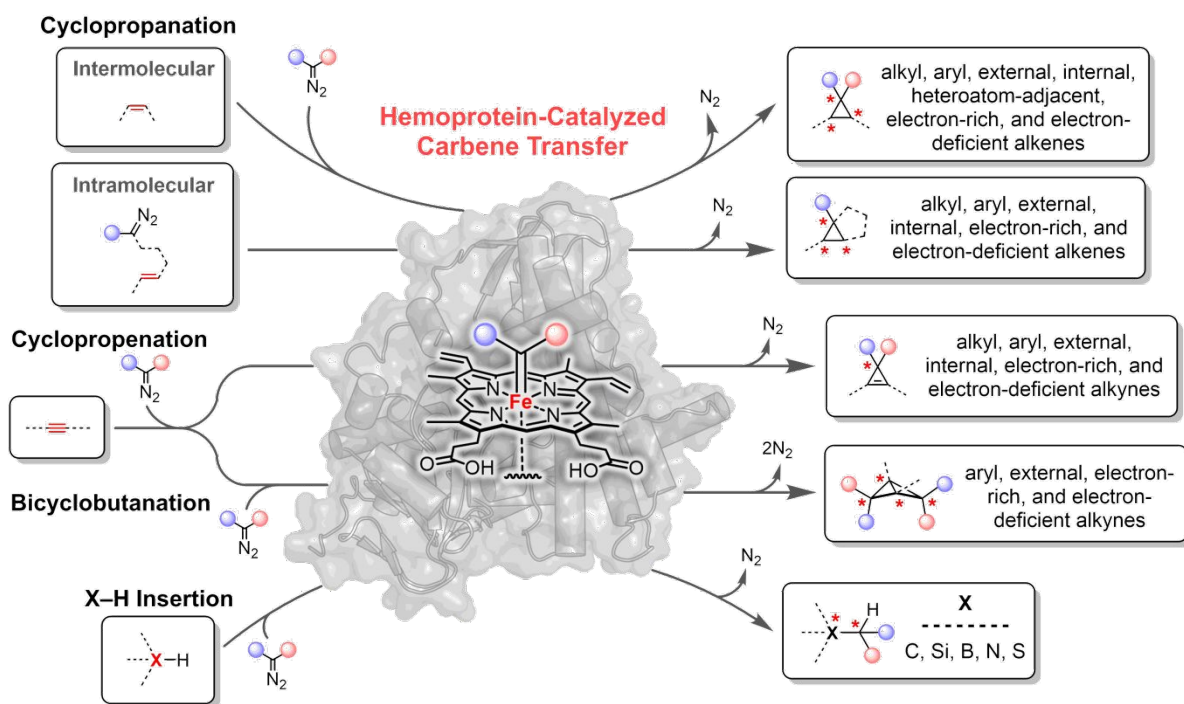


Figure 3. Summary of abiological carbene-transfer reactions catalyzed by hemoproteins. The red asterisks indicate possible chiral centers in the reaction products; the red and blue spheres indicate the possibility of variable functional groups originating from the diazo-bearing substrates.

These pioneering studies opened the floodgates to a wave of abiological reactions catalyzed by hemoproteins (**Figure 3**), of which many sport substitutions of key active-site residues distinguished by mechanistic research. A pool of olefin cyclopropanation catalysts has now been engineered to address several reactivity and selectivity challenges within the context of this valuable transformation.⁶⁶⁻⁷⁸ The concept of carbene transfer to π systems has also been expanded to include alkyne substrates, from which the highly strained cyclopropene and bicyclobutane products are furnished in high yield and with excellent selectivity.^{79,80} Additionally, hemoproteins

have been engineered for insertion of carbenes into N–H,^{81,82} S–H,^{68,83} Si–H,⁸⁴ and B–H bonds.⁸⁵⁻⁸⁷ These advancements recently culminated in P411 enzymes proficient at inserting carbenes into C(*sp*³)–H bonds,⁸⁸⁻⁹⁰ a reaction with enormous potential to transform the way we construct C–C bonds.

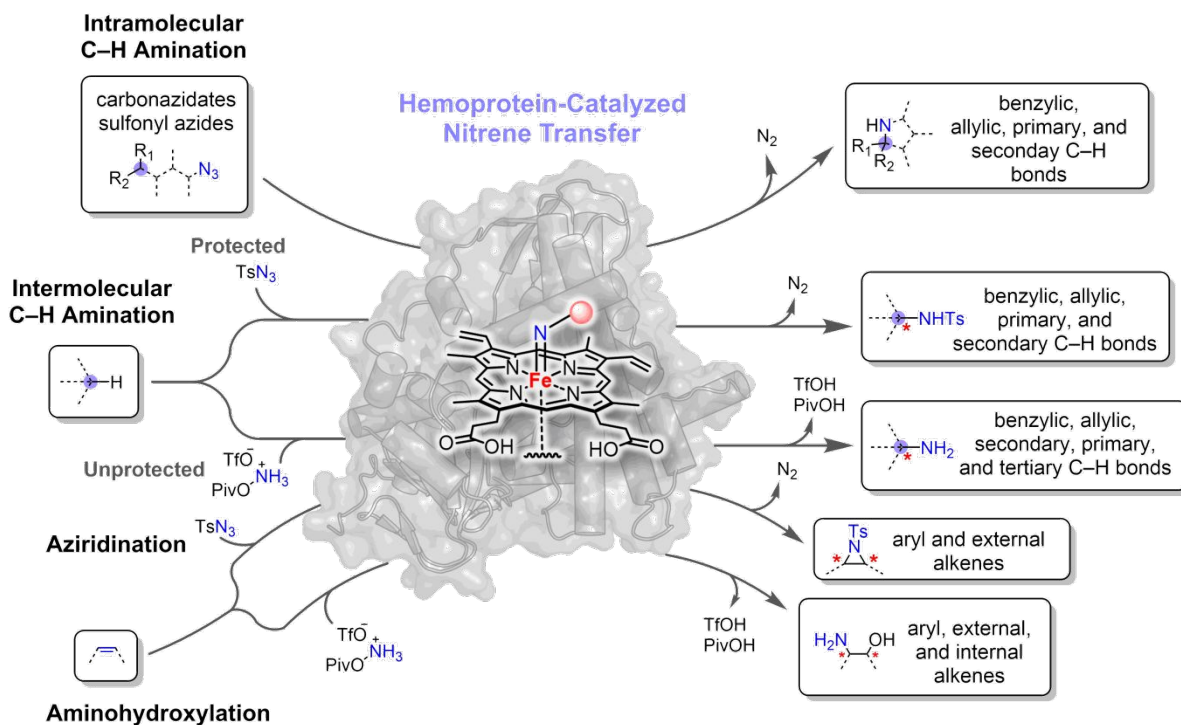


Figure 4. Summary of abiological nitrene-transfer reactions catalyzed by hemoproteins. The red asterisks indicate possible chiral centers in the reaction products.

Hemoproteins have also been discovered and engineered to act as efficient transferases of nitrene intermediates, similar to carbenes. That hemoproteins could insert nitrene intermediates into C–H bonds was shown as far back as 1985.⁹¹ It was not until 28 years later, however, that this reactivity was exploited and improved upon by directed evolution to achieve multiple turnovers (**Figure 4**). McIntosh, Coelho, and coworkers demonstrated that a cyclopropanating enzyme, P411_{BM3}-CIS, could catalyze an intramolecular C–H amination reaction of the 2,4,6-

1
2
3 triethylbenzene-1-sulfonyl azide nitrene precursor (wherein the loss of N₂ drives formation of an
4 iron-nitrenoid, analogous to the carbene-transfer reaction) with up to 680 TTN;⁹² Singh and
5 coworkers engineered P450s for a similar purpose.⁹³ An intermolecular version of this reaction
6 was later established with tosyl azide and 4-ethylanisole.⁹⁴ Aziridination of olefin substrates was
7 also achieved with engineered P411 catalysts, using the same nitrene precursor.⁹⁵ Recent advances
8 in synthetic methodology,⁹⁶ and subsequent discovery of a natural P450 nitrene transferase,
9 BezE,⁹⁷ however, inspired researchers in our laboratory to turn to hydroxylamine esters as a nitrene
10 source, which could furnish unprotected amine products in a single step. Engineered hemoproteins
11 were active with these nitrene precursors in the asymmetric aminohydroxylation of olefin
12 substrates, the top variants exhibiting impressive levels of activity and selectivity.⁹⁸ More recently,
13 a lineage of P411s was engineered to insert these unprotected nitrenes directly into primary,
14 secondary, and tertiary C(*sp*³)-H bonds, an invaluable transformation that currently has no
15 synthetic counterpart.⁹⁹

16
17 Throughout this expansion of carbene- and nitrene-transfer reactions catalyzed by
18 hemoproteins, the choice of hemoprotein has also grown. P450s, cytochromes *c*,⁸⁴ myoglobins,⁷⁰
19 protoglobins,⁶⁶ and a nitric oxide dioxygenase (NOD)⁶⁶ have all served as starting points for site-
20 specific mutagenesis or directed evolution to engineer more active and more selective biocatalysts.
21 Furthermore, an assortment of both natural and noncanonical amino acids has been explored as
22 axial ligands to the heme.¹⁰⁰ Following the Hilvert Lab's discovery that an *N*-methyl-His axial
23 ligand enhanced the native reactivity of ascorbate peroxidase and the peroxidase activity of
24 myoglobin,^{101,102} Carminati and Fasan demonstrated that a myoglobin variant presenting this
25 noncanonical amino acid to a synthetic iron-2,4-diacetyl deuteroporphyrin IX cofactor catalyzed
26 the cyclopropanation of both electron-rich and electron-poor olefins, of which the latter had

1
2
3 remained a challenging substrate for such biocatalytic transformations.⁷⁵ Interestingly, their
4 experimental observations suggested that the reaction mechanism had been altered, and now
5 proceeded down a stepwise radical pathway rather than the previously hypothesized concerted
6 carbene-transfer pathway. We anticipate more such observations as the hemoprotein platform is
7 pushed in creative new directions to overcome contemporary synthetic challenges.
8
9

10
11
12
13
14
15 The studies recounted above demonstrate how iron-carbenoid and iron-nitrenoid
16 intermediates within an enzyme active site can be channeled toward the construction of useful
17 bonds, but these highly reactive species can also escape down reaction pathways that generate
18 undesirable side products. In carbene-transfer reactions, alkylation of the heme cofactor or nearby
19 protein residues is a limiting factor in maximizing catalytic turnovers.¹⁰³ While this side reaction
20 is also possible in nitrene-transfer reactions, reduction of the nitrene to a primary amine is perhaps
21 the most problematic side pathway, particularly in the context of intermolecular reactions.^{94,104} In
22 both carbene- and nitrene-transfer reactions, substrates bearing multiple modes or sites of
23 reactivity further exacerbate this problem, as additional pathways of intermediate decay can result
24 in diminished chemo-, regio-, and stereoselectivity. While these obstacles should always be
25 considered when embarking on a new reaction, it is worth recognizing the benefits imparted by a
26 mutable protein scaffold: in many of the carbene-transfer and virtually all of the nitrene-transfer
27 reactions described to date, the free heme cofactor fails to produce measurable quantities of the
28 desired products. And, in the cases where activity is observed, the TTNs and enantiomeric excesses
29 pale in comparison to those with the engineered hemoproteins. In summary, the laboratory-evolved
30 protein architecture plays a crucial role in directing reactive intermediates along the desired
31 reaction pathways, much the same way that the natural versions of these cytochromes P450 direct
32 compounds I and II.
33
34
35
36
37
38
39
40
41
42
43
44
45
46
47
48
49
50
51
52
53
54
55
56
57
58
59
60

3. NONHEME IRON

3.1. Reactions of Ferrous Iron with Oxygen Species

Ferrous iron alone can also be a catalyst in reactions with various oxygen species. Although the oxidation of Fe(II) to Fe(III) in the presence of O₂ in aqueous solutions generally leads to the undesired precipitation of ferric hydroxide complexes, especially in alkaline solutions, other conditions that promote useful iron-catalyzed reactions have been described. In the Fenton reaction, for instance, Fe(II) disproportionates H₂O₂ to HO• and HOO•, and produces H₂O as a byproduct.¹⁰⁵ The resulting radical species can then oxidize organic compounds, which is the basis of the reaction's application to the purification of groundwater and soils contaminated with hydrocarbons.¹⁰⁶ Fe(II) in the presence of peroxy acids is converted to the Fe(IV)-oxo (ferryl) intermediate, which was demonstrated to catalyze C–H oxidation reactions that later helped establish the stepwise model (HAT and oxygen rebound) for many biological oxidations.^{107,108} Reaction of aqueous Fe(II) with ozone (O₃) also produces the reactive ferryl species.¹⁰⁹ Under these conditions, ketones and other byproducts were generated from one- and two-electron oxidations of cyclic alcohols.¹¹⁰ In the Gif oxygenation systems, these ferryl species are formed directly from O₂ in the presence of reductants (Zn or NaS) and pyridine.¹¹¹⁻¹¹³ While the culmination of this body of work has indeed yielded catalytic systems that can functionalize strong C–H bonds, many of these fundamentally important reactions suffer from unproductive oxidation and precipitation of the catalyst, a general lack of control over intermediary radical species, and limited regio- and stereoselectivity, hindering their applications more broadly.

Nonheme iron-dependent oxygenases, however, effect similar C–H functionalization reactions efficaciously by protecting the ferrous cofactor from unproductive oxidation, tuning reactivity with O₂, and positioning substrates such that reactive intermediates are guided down the desired pathway. Here, we narrow our focus to mononuclear Fe(II)-dependent oxygenases that

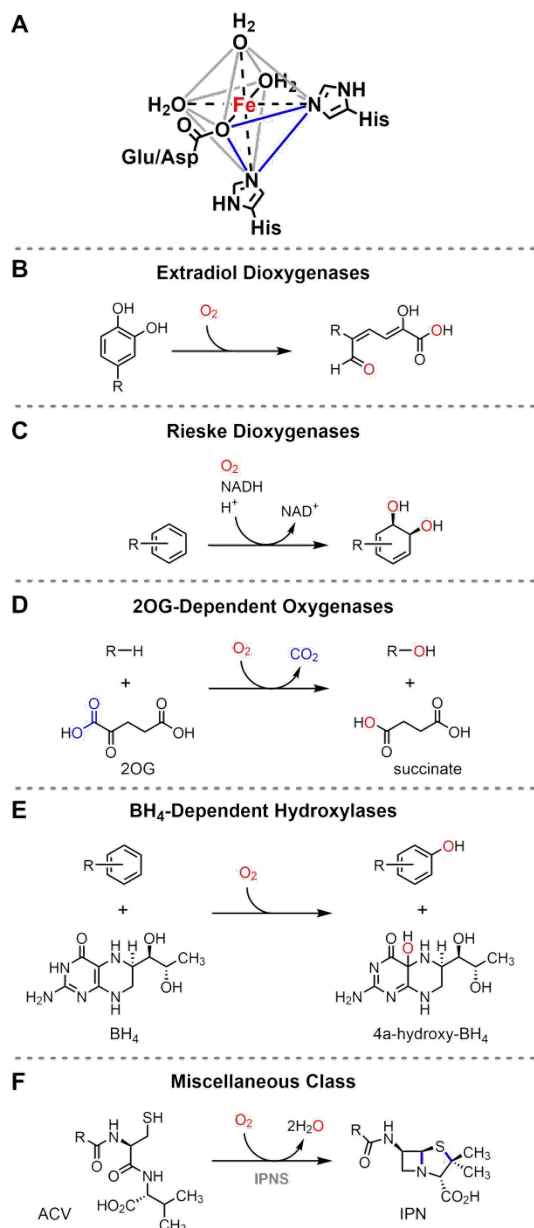


Figure 5. A, The 2-His-1-carboxylate facial triad iron-binding motif. The vertices of one face of the octahedron are occupied by the three protein ligands (blue triangle). The general reactions catalyzed by each of the 2-His-1-carboxylate enzyme families are shown in **B-F**. The conversion of δ -(L- α -aminoadipoyl)-L-cysteinyl-D-valine (ACV) to isopenicillin *N* by the oxidase IPNS is a representative example in the miscellaneous class, which includes oxygenases, oxidases, and peroxidases.

employ the 2-His-1-carboxylate iron-binding motif. These enzymes catalyze a remarkable diversity of oxidative transformations stemming from this ostensibly simple, earth-abundant metal, providing another example of how the protein environment can modulate cofactor reactivity and maximize its catalytic potential.

3.2. C–H Oxidation Reactions Catalyzed by 2-His-1-Carboxylate Enzymes

2-His-1-carboxylate enzymes activate O₂ for a diversity of C–H oxidation reactions with an iron-binding motif comprised of two histidines and one glutamate or aspartate.^{2,114-116} This facial triad of protein ligands occupies the vertices of one face of the octahedral iron, leaving open three coordination sites for waters, substrates, co-substrates, and various species of oxygen (**Figure 5A**).

Because of the divergence in requirements for additional co-substrates and cofactors, enzymes that utilize this motif are divided into the following five families: the extradiol dioxygenases (**Figure 5B**),¹¹⁷ the Rieske dioxygenases (**Figure 5C**),¹¹⁸ the 2-oxoglutarate

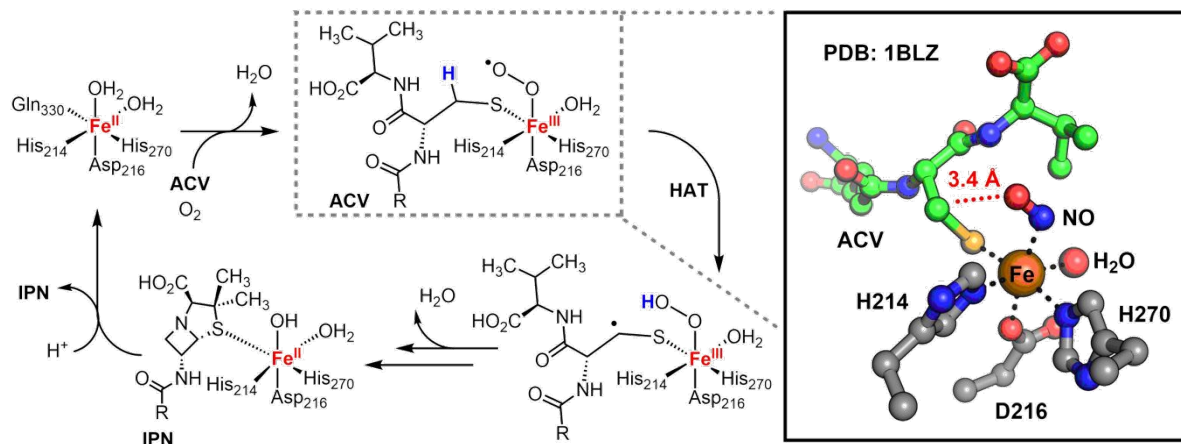


Figure 6. Abbreviated mechanism of the conversion of L- δ -aminoadipoyl-L-Cys-D-Val (ACV, green) to isopenicillin *N* (IPN) catalyzed by IPNS. The crystal structure of the NO-bound complex (right, PDB: 1BLZ), a mimic of the HAT-initiating ferric superoxide intermediate, demonstrates how the protein-enforced orientation of the iron-bound substrate results in productive reactivity.

(2OG)-dependent oxygenases (**Figure 5D**),¹¹⁹ the tetrahydrobiopterin (BH₄)-dependent hydroxylases (**Figure 5E**),¹²⁰ and a miscellaneous class that includes isopenicillin *N*-synthase (IPNS),^{121,122} (*S*)-2-hydroxypropyl-1-phosphonate epoxidase (HppE),¹²³ 2-hydroxyethylphosphonate dioxygenase (HEPD),¹²⁴ methylphosphonate synthase (MPnS) (**Figure 5F**),¹²⁵ and 1-aminocyclopropane-1-carboxylate oxidase (ACCO).¹²⁶ The references logged above

129

Despite the catalytic diversity of 2-His-1-carboxylate enzymes, a general strategy to regulate entry into the reaction cycle has emerged. The ferrous resting state of the cofactor renders it, in principle, highly susceptible to unproductive oxidation, necessitating a mechanism to protect the active site during periods of inactivity. Similar to P450s (*vide supra*), the binding of substrates

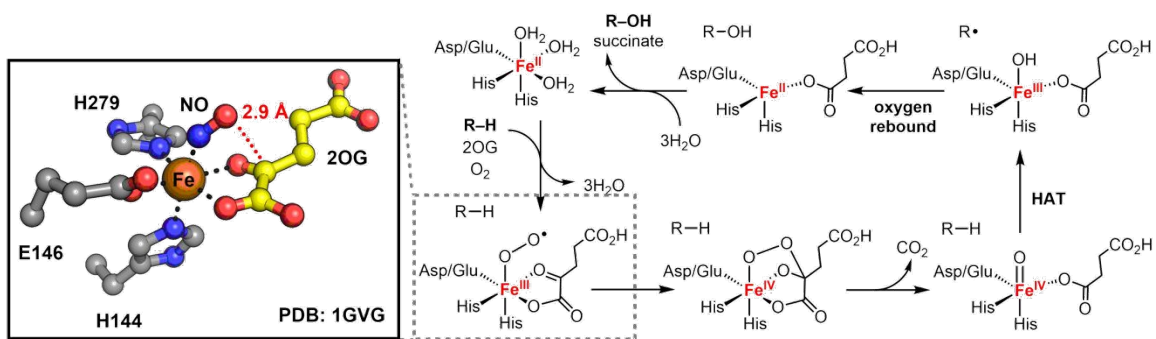


Figure 7. Established mechanism of aliphatic C–H hydroxylation catalyzed by 2OG-dependent oxygenases. The NO-bound crystal structure of CAS1 (left, PDB: 1GVG) shows a close proximity of the distal oxygen of the ferric superoxide intermediate to C2 of 2OG (yellow), leading to oxidative cleavage of the co-substrate to succinate and CO₂, and ultimately hydroxylation of the primary substrate.

triggers the dissociation of one or more coordinated water molecules, constituting a protein-controlled shift in the ligand sphere to promote a five-coordinate Fe(II) center, which opens a site for binding of O₂.^{2,115} The displacement of water with anionic ligands is also thought to decrease the Fe(III/II) reduction potential for productive oxidation of the cofactor.¹¹⁵ Whereas the substrates or co-substrates of the extradiol dioxygenases, 2OG-dependent oxygenases, and IPNS fill this role by directly coordinating to the iron,^{117,119,130} the BH₄-dependent hydroxylases and Rieske dioxygenases, whose substrates contribute no additional anionic ligands, effect a similar outcome by bidentate coordination of the protein's carboxylate ligand.^{118,120}

The steps following substrate binding and O₂ activation in each of the 2-His-1-carboxylate families diverge, giving rise to an assortment of structurally and electronically distinct intermediates. Nevertheless, a unifying theme concerning the protein's influence over the reaction progression is clear: the polypeptide scaffold binds the substrate, co-substrate, or additional cofactor involved in the subsequent step in an orientation that encourages productive interaction with the intermediary iron-bound oxygen species. In IPNS, the end-on ferric superoxide initiates a HAT from the substrate C–H bond neighboring the iron-coordinated thiolate, the committed step

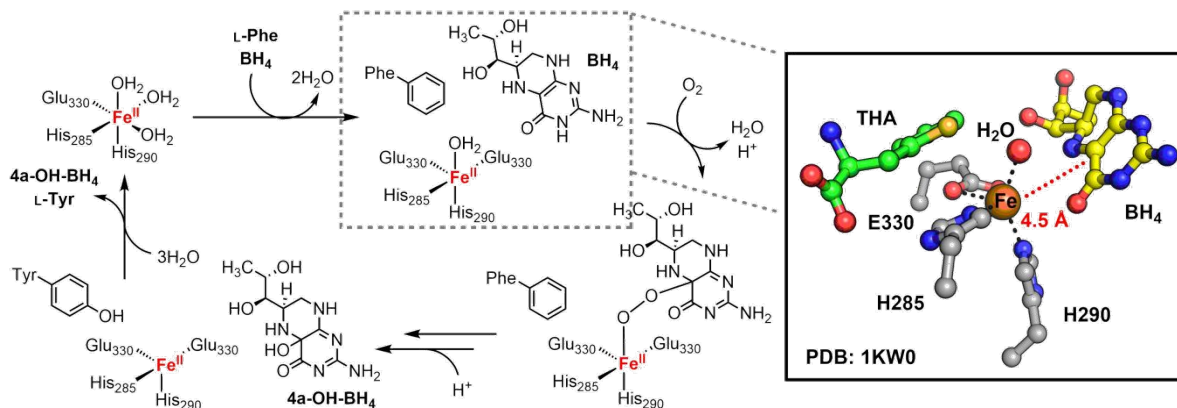


Figure 8. Abbreviated mechanism of the conversion of L-phenylalanine to L-tyrosine catalyzed by phenylalanine hydroxylase. The BH₄-bound crystal structure with the 3-(2-thienyl)-L-alanine (THA, green) substrate analogue (right, PDB: 1KW0) shows how the protein orients the two cofactors in such a way to achieve reductive cleavage of O₂ and oxidation of the aromatic substrate.

leading to C–N and C–S bond formation.¹²² The juxtaposition of the implicated atoms was shown clearly in the NO-bound crystal structure (PDB: 1BLZ), wherein the distal oxygen of the O₂ surrogate is in close proximity to the target carbon (**Figure 6**).¹³⁰ Similar observations were made in the NO-bound crystal structures of the 2OG-dependent enzymes clavamate synthase I (CAS1, PDB: 1GVG) and WelO5 (PDB: 5IQV).^{131,132} In these cases, however, the distal oxygen of the O₂ surrogate is poised to attack C2 of the co-substrate 2OG, which ultimately provokes O–O bond

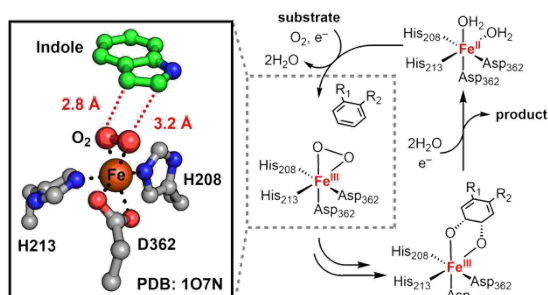
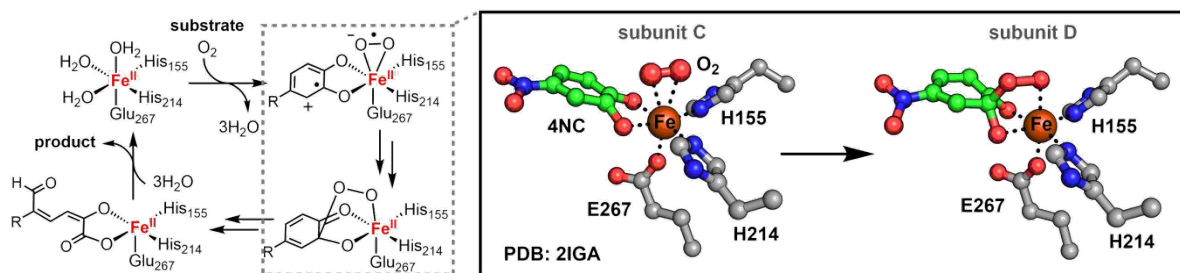


Figure 9. A side-on binding orientation of O₂ to the iron cofactor in the Rieske dioxygenase family, as observed in the crystal structure of NDO (left, PDB: 1O7N) with the indole substrate analogue (green), results in *syn*-hydroxylation of aromatic substrates.

scission and ferryl formation (**Figure 7**). In the BH₄-dependent hydroxylases, a bridged Fe(II)–O–O–BH₄ intermediate is thought to precede ferryl formation and substrate oxidation, again necessitating a propinquity of the two cofactors.^{133,134} Indeed, this was observed in a crystal structure of the phenylalanine hydroxylase ternary complex with the 3-(2-

1
2
3 thienyl)-L-alanine (THA) substrate analogue (PDB: 1KW0, **Figure 8**).¹³⁵ The Rieske and extradiol
4 dioxygenases leverage a side-on binding mode of O₂ to affect product formation. In the former
5
6 dioxygenases leverage a side-on binding mode of O₂ to affect product formation. In the former
7
8 family, the orientation of the substrate results in *syn*-hydroxylation of the aromatic system, as was
9
10 revealed by the crystal structures of naphthalene dioxygenase (NDO, PDB: 1O7N) and carbazole
11
12 1,9a-dioxygenase (CARDO, PDB: 3VMI) bearing the intermediate state (**Figure 9**).^{136,137} In the
13
14 latter family, a single crystal structure depicting multiple states of the homoprotocatechuate 2,3-
15
16 dioxygenase (2,3-HPCD, PDB: 2IGA) reaction cycle demonstrates how the cofactor-substrate
17
18 relationship promotes substrate-driven reduction of O₂ and eventually cleavage of the aromatic
19
20 ring (**Figure 10**).¹³⁸ In a more recent study on 3-hydroxyanthranilate-3,4-dioxygenase (HAO), a
21
22 close relative of the extradiol dioxygenases, an astonishing seven states of the reaction cycle were
23
24 captured by x-ray crystallography.¹³⁹ Although this enzyme does not appear to bind O₂ in the same
25
26 side-on orientation, the protein scaffold still guides the reaction through a similar course of events.

27
28
29
30
31 Several of the 2-His-1-carboxylate families form high-valent ferryl intermediates for the
32
33 cleavage of strong C–H bonds.¹⁴⁰ Unlike those formed free in solution, these enzymatic
34
35



48
49
50
51
52
53
54
55
56
57
58
59
60

Figure 10. Abbreviated mechanism of the cleavage of catechol substrates catalyzed by members of the extradiol ring-cleaving dioxygenase family. The side-on binding mode of O₂ observed in the crystal structure of 2,3-HPCD (right, PDB: 2IGA) positions the intermediate close to the correct carbon of the 4-nitrocatechol substrate (4NC, green), which results in substrate-driven reduction of O₂ and ultimately insertion of both oxygens into product structure. Remarkably, multiple states of this reaction cycle were captured in different subunits of the asymmetric unit in the same crystal sample.

intermediates are channeled with precise stereoelectronic control. 2OG-dependent oxygenases, in particular, are a testament to such precise channeling, as ferryl-mediated C–H activation leads to an astounding diversity of transformations that, in most instances, are catalyzed with exceptional selectivity.¹⁴¹ In this family, the reduction of O₂ and oxidative conversion of 2OG to succinate and CO₂ results in ferryl formation,¹⁴²⁻¹⁵² which then effects C–H bond cleavage to yield ferric-hydroxide and substrate-centered radical intermediates, a key branchpoint in 2OG-dependent oxygenase catalysis. The origin of chemoselectivity stemming from this state has been studied extensively by dissecting and comparing the mechanisms employed by the hydroxylase and halogenase subfamilies. In the hydroxylation pathway, oxygen rebound furnishes the product and regenerates the Fe(II) cofactor for subsequent turnovers (**Figure 7**), similar to P450-catalyzed hydroxylation reactions.^{18,119} In the halogenation pathway, a *cis*-coordinated halogen is transferred (Cl• or Br•) in lieu of the hydroxyl group (**Figure 11**). This transfer is first enabled by substitution of the iron-binding carboxylate ligand of the facial triad for an alanine or glycine, as demonstrated by the substrate-free crystal structure of the carrier-protein-dependent chlorinase SyrB2 (PDB:

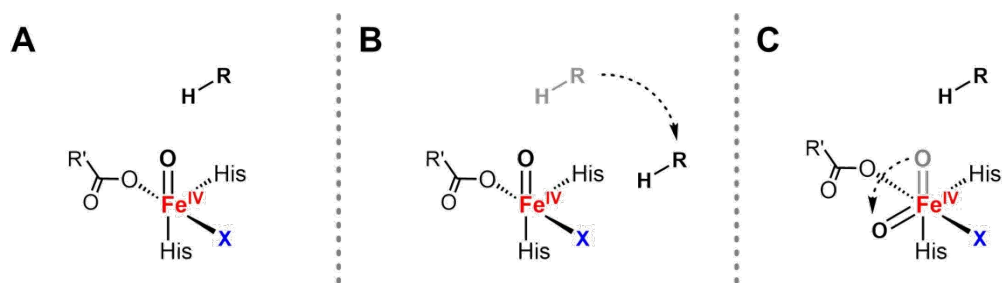


Figure 11. Comparative models showing the generalized protein-dictated orientations of the substrate and ferryl intermediate in 2OG-dependent enzyme catalysis. The inline ferryl with substrate bound directly above the oxo is the typical configuration for hydroxylation (**A**). Halogenation is achieved by binding the substrate such that rebound of the halogen radical is favored (**B**), or by reorientation of the ferryl to disfavor oxygen rebound (**C**). The blue **X** represents an iron-coordinated aspartate, glutamate, or halide; the substrate is depicted as R–H; the gray R–H and iron–oxo bond are shown to illustrate the change in position of the respective species, not to be interpreted as being present in the complex.

1
2
3 2FCV and 2FCT), wherein the halide coordinates directly to the cofactor.¹⁵³ Further dissection of
4
5 the SyrB2 reaction placed crucial importance on the substrate-cofactor disposition to achieve a
6
7 selective halogenation outcome (**Figure 11B**).¹⁵⁴⁻¹⁵⁶ More recently, structural studies on the
8
9 chlorinase WelO5 presented an alternative strategy to effect halogenation: a protein-controlled
10
11 rearrangement of the ferryl intermediate properly juxtaposes the substrate and cofactor for
12
13 selective halogen transfer (**Figure 11C**).¹³² In both cases, subtle yet precise effects of the protein
14
15 environment seem to dictate the preference for rather disparate outcomes, a premise that is also
16
17 relevant to the desaturation,¹⁵⁷ epoxidation,^{152,158} cyclization,^{150,159,160} epimerization,¹⁴⁸ and
18
19 endoperoxidation¹⁶¹ reactions catalyzed by this family.
20
21
22
23
24
25

26 **3.3. The Facial Triad Supports Abiological Activity**

27 The astonishing catalytic repertoire of nonheme iron-dependent oxygenases, oxidases, and
28
29 peroxidases bearing the 2-His-1-carboxylate facial triad has inspired researchers to investigate
30
31 whether this enzymatic platform could be extended to useful abiological transformations. While
32
33 this vision has indeed proven to be possible, the collection of engineered catalysts is still in its
34
35 infancy. However, the future is nonetheless bright for this family of enzymes, and we anticipate
36
37 that the progress summarized below is just the beginning.
38
39
40

41 Members of the 2OG-dependent halogenase subfamily hold great biocatalytic potential
42
43 within the confines of their native catalytic function, as there is currently a paucity of methods to
44
45 directly halogenate aliphatic C–H bonds with a high degree of selectivity.¹⁶²⁻¹⁶⁶ Our understanding
46
47 of these enzymes also led some researchers to investigate whether other anionic species that would
48
49 likely coordinate to the cofactor could be coupled to intermediate substrate radicals via an
50
51 analogous mechanism. Indeed, trace levels of nitration and azidation activity were detected in
52
53 SyrB2 preparations with the native substrate and substrate analogues, constituting an important
54
55
56
57

1
2
3 Azide-bearing amino acids have also been explored as substrates for 2OG-dependent
4 oxygenases. In a recent study, the native hydroxylases PolL and LdoA catalyzed the oxidative
5 conversion of these azidated substrates to nitrile products (**Figure 12B**).¹⁷² Further investigation
6 demonstrated the requirement of both O₂ and 2OG, suggesting that the reaction still proceeds by
7 ferryl formation and HAT, and that the azido moiety acts as an assisting group. A similar finding
8 was also reported in the Rieske dioxygenase family, wherein toluene dioxygenase (TDO)
9 converted a benzyl azide to a benzyl nitrile.¹⁷³ In both cases, iron-nitrenoid intermediates were
10 proposed as a possible branchpoint after substrate hydroxylation.
11
12
13
14
15
16
17
18
19
20

21 Goldberg, Knight, and coworkers recently demonstrated that similar iron-nitrenoid
22 intermediates could effect nitrene-transfer reactions (**Figure 12C**) analogous to those catalyzed by
23 engineered hemoproteins (*vide supra*).¹⁷⁴ Activity for the intermolecular aziridination of styrene
24 and the intramolecular benzylic C–H insertion of 2-ethylbenzenesulfonyl azide was detected with
25 the 2OG-dependent ethylene-forming enzyme (EFE). EFE variants exhibiting improvements in
26 both activity and stereoselectivity were obtained by directed evolution, establishing that this family
27 of enzymes can also be tuned for abiological catalysis. A subsequent study by Vila, Steck, and
28 coworkers suggests that nitrene transferase activity may be a common side reactivity of 2-His-1-
29 carboxylate enzymes, as various 2OG-dependent oxygenases and Rieske dioxygenases were also
30 shown to facilitate similar nitrene-transfer reactions.¹⁷⁵
31
32
33
34
35
36
37
38
39
40
41
42
43

44 The presence of multiple iron coordination sites left unoccupied by protein ligands creates
45 attractive opportunities for engineering this enzymatic platform using exogenous ligands to tune
46 the reactivity of the cofactor (**Figure 5A**). Indeed, Goldberg and Knight discovered the native co-
47 substrate, 2OG, of EFE enhanced the activity of the aziridination and C–H insertion reactions with
48 both the native and engineered versions of the enzyme.¹⁷⁴ Other anionic ligands, such as acetate
49
50
51
52
53
54
55
56
57
58
59
60

1
2
3 and *N*-oxalylglycine (NOG), further boosted the activity of both reactions and improved the
4 chemoselectivity of the C–H insertion reaction. Although they did not determine the mechanisms
5 of these enhancements, their observations demonstrate that exogenous ligands are a further handle
6 for tuning novel reactivities. This expanded access to the iron provides an additional, flexible
7 component upon which the protein scaffold can draw to guide reactive intermediates down new
8 pathways.
9

19 **4. ENGINEERING THE FUTURE**

21 **4.1. From Comprehension to Application**

22 The machinery of natural enzymes has fueled the imagination of researchers for decades. But is
23 an understanding of mechanism a prerequisite to engineering an abiological function? Luckily, the
24 answer is no. While the disparities between our understanding of the chemistry occurring at the
25 enzyme active site and the astounding complexity of interactions that contribute to protein folding,
26 dynamics, and catalysis preclude us from designing most new biocatalysts *de novo* (at least for the
27 time being), we can engineer new enzymes from existing scaffolds even if the intricacies of such
28 scaffolds cannot be fully deconstructed. Nevertheless, knowledge gained from mechanistic
29 studies, while not strictly required, can certainly assist in discovering new reactivities and
30 streamlining engineering processes such that desired catalytic enhancements can be achieved on
31 reasonable timescales. To bridge the gap between comprehension and application, we introduce
32 the challenges of engineering natural enzymes for abiological chemistry, and then provide
33 examples of how mechanistic knowledge of both natural and laboratory-evolved enzymes has
34 guided protein engineers in tuning iron-dependent oxygenases.
35
36
37
38
39
40
41
42
43
44
45
46
47
48
49
50
51

52 From controlling the flow of electrons and protons to protecting the active-site architecture
53 from oxidative inactivation, natural evolution has honed iron-dependent oxygenases into
54
55
56
57

1
2
3 sophisticated molecular machines. The driving force behind this process is the selective advantage
4 conferred by the products, which promote the survival of an organism bearing mutations that
5 enhance the reaction outcome. Over time, this selective pressure can furnish a highly refined
6 enzyme. In the context of evolving a biocatalyst for an abiological reaction, the protein engineer
7 must first discover an enzyme exhibiting measurable activity for the desired reaction, generate
8 mutants of this parent enzyme, and then foster the desired outcome by compounding beneficial
9 mutations and rejecting mutations that fail to yield improvements.¹⁷⁶ In principle, this process
10 could produce enzymes comparable to the products of natural evolution. In practice, however, time
11 constitutes a major limitation: screening the entire landscape of possible mutations in the context
12 of even the smallest of proteins is impracticable. Moreover, many abiological reactions cannot be
13 coupled to the fitness of an organism, or the products fail to produce a distinctive fluorogenic
14 handle that would allow for rapid detection. Most efforts necessitate use of more time-intensive
15 analytical techniques that decrease capacity to screen sequences (e.g., liquid and gas
16 chromatography). Consequently, we resort to strategies to create smarter, experimentally tractable
17 libraries that allow us to climb local fitness peaks (e.g., site-saturation mutagenesis).¹⁷⁷ Although
18 such a process will likely miss out on some of the characteristics that make natural enzymes so
19 powerful, the results are nonetheless impressive.
20
21
22
23
24
25
26
27
28
29
30
31
32
33
34
35
36
37
38
39
40
41

42 An understanding of natural enzyme mechanism, even one that is rudimentary, can point
43 the engineer to specific residues or regions of a protein structure that are important to catalysis.¹⁷⁸
44 This knowledge can then be applied to the design of libraries for engineering. In the context of
45 iron-dependent oxygenases, this is clearly exemplified in the transformation of P450_{BM3} to
46 P411_{BM3} (*vide supra*): although the entirety of the contemporary P450 C–H activation model was
47 likely superfluous, knowledge of the axial ligand's electronic effects on the heme cofactor was
48
49
50
51
52
53
54
55
56
57
58
59
60

1
2
3 pivotal to the discovery of P450_{BM3} variants that exhibited redox potentials suited for
4
5 cyclopropanation in whole cells.⁶⁵ Likewise, crystal structures of the P450_{BM3} heme domain and
6
7 engineered variants thereof have aided numerous other directed evolution campaigns in the
8
9 exploration of the platform's ability to catalyze abiological reactions.^{65,94,179}
10
11

12 Mechanistic investigations of laboratory-evolved variants can also confer useful
13
14 information for the design of smarter libraries. A recent study of *Rhodothermus marinus*
15
16 cytochrome *c* engineered for C–Si and C–B bond formation yielded a crystal structure with an iron
17
18 porphyrin-bound carbene intermediate.¹⁸⁰ The structure revealed how mutations to a surface loop
19
20 region rendered it more flexible than that of the native enzyme, an observation that was leveraged
21
22 to engineer a C–B bond-forming enzyme capable of accepting diverse trifluorodiazole alkane
23
24 carbene precursors to furnish the corresponding α -trifluoromethylated organoborane products.⁸⁷
25
26 Site-saturation libraries focused on this region yielded multiple beneficial mutations, and the final
27
28 variant maintained levels of activity and selectivity with a trifluorodiazole alkane substrate scope
29
30 comparable to the model reaction. Computational analysis of the engineered enzyme supported the
31
32 original mechanism-driven hypothesis: the heme-binding pocket positioned the iron-carbenoid
33
34 intermediate such that the pro-*R* face was exposed to the putative borane-binding pocket, while the
35
36 variable alkyl substituent was arranged to have a minimal effect on the reaction outcome.⁸⁷
37
38
39
40
41

42 Although the finer details of our mechanistic knowledge oftentimes lack a direct
43
44 application to the engineering process, it is difficult to imagine a world where we climb to the
45
46 same peaks of ingenuity without the contributions from mechanistic enzymology. It is even
47
48 conceivable that some of these recent innovations, and those still to be described, already exist in
49
50 the biological world, which will render their eventual discoveries all the more enchanting.
51
52
53
54

55 **4.2. Iron-Dependent Oxygenases in Organic Synthesis**

56
57

1
2
3 We are optimistic that applications of iron-dependent biocatalysts as real-world synthetic tools
4 will grow, as the expansion of methods to selectively functionalize C–H bonds will certainly have
5 an impact on both the *de novo* synthesis and late-stage modification of drug compounds and
6 potentially therapeutic natural products. The native oxidative functions of P450s have already been
7 applied to such goals, whether in the hydroxylation of steroids and other useful organic
8 molecules,^{181,182} or more recently in the chemoenzymatic syntheses of nigelladine A and several
9 meroterpenoid natural products.^{183,184} Likewise, native 2OG-dependent hydroxylases and
10 halogenases have been utilized by the Renata Lab and others in the synthesis and tailoring of
11 natural product compounds.¹⁸⁵⁻¹⁹⁵ A few examples of the abiological transformations enabled by
12 these platforms have already surfaced: the cyclopropyl core structures of the approved drugs
13 levomilnacipran, ticagrelor, tranylcypromine, and tasimelteon, as well as a TRPV1 antagonist drug
14 candidate, have been constructed with engineered P450s and globins.¹⁹⁶⁻¹⁹⁸

15
16
17
18
19
20
21
22
23
24
25
26
27
28
29
30
31 Enzyme engineers ultimately aspire to see the products of their creativity and labor used
32 directly in the manufacture of valuable compounds. Industrial-scale processes, however, require
33 much more than exciting new reactivity. Space-time yield ($\text{g L}^{-1} \text{h}^{-1}$) of the desired product is a
34 key metric of overall performance, to which the activity, specificity, and stability of the enzyme
35 are all contributing factors. From a protein engineering standpoint, advances in both experimental
36 technologies and computational methods—to effectively increase screening capacity and narrow
37 library sizes, respectively—will better equip us to navigate complex fitness landscapes and reach
38 these requisite fitness peaks. However, other factors in the process must also be considered,
39 including substrate and product titers, solvent compatibility with upstream and downstream steps,
40 and isolation of the products in pure form. The challenges associated with incorporating
41
42
43
44
45
46
47
48
49
50
51
52
53
54
55
56
57
58
59
60

1
2
3 biocatalysts into industrial processes and realistic approaches moving forward have been the
4
5 subjects of several recent and comprehensive reviews.¹⁹⁹⁻²⁰²
6
7
8
9

10 **5. CONCLUDING REMARKS**

11
12 Until the day when computational methods and *de novo* protein design can furnish biocatalysts
13
14 capable of fulfilling our demands, leveraging our understanding of natural enzymes toward
15
16 discovery and evolution of new functions remains a fruitful approach to the development of useful
17
18 synthetic tools. Nature's catalytic machinery has energized the scientific community for centuries,
19
20 and engineered versions of enzymes have now expanded the pool from which to draw inspiration.
21
22 As in all disciplines of science, collaboration is crucial. The convergence of enzymology, synthetic
23
24 chemistry, computation, and engineering is the motor that drives forward the field of biocatalysis.
25
26
27
28
29
30

31 **AUTHOR INFORMATION**

32 **Corresponding Author**

33
34 **Frances H. Arnold** – Division of Chemistry and Chemical Engineering, California Institute
35 of Technology, Pasadena, California 91125, United States; orcid.org/0000-0002-4027-364X;
36 *Email: frances@cheme.caltech.edu
37
38

39 **Authors**

40 **Noah P. Dunham** – Division of Chemistry and Chemical Engineering, California Institute of
41 Technology, Pasadena, California 91125, United States; orcid.org/0000-0001-8006-9566
42

43 **Notes**

44
45 The authors declare no competing financial interest.
46
47
48

49 **ACKNOWLEDGEMENTS**

50
51 This work was supported by the US Army Research Office Institute for Collaborative
52 Biotechnologies contract W911NF-19-D-0001 and the Joseph J. Jacobs Institute for Molecular
53 Engineering for Medicine. N.P.D. was supported by the Ruth L. Kirschstein NIH Postdoctoral
54 Fellowship (F32GM131620). We thank Professor Haoming Zhang for providing the open- and
55 closed-state coordinates resulting from the full-length P450_{BM3} cryo-EM structures. We also thank
56
57

1
2
3 Dr. S. V. Athavale, Dr. D. C. Miller, and Dr. Z. Liu for providing helpful comments on the
4 manuscript.
5
6
7

8 REFERENCES 9

- 10 (1) Silverman, R. B. Enzymes as Catalysts. In *Organic Chemistry of Enzyme-*
11 *Catalyzed Reactions (Second Edition)*; Academic Press: San Diego, 2002, p 1-38.
- 12 (2) Solomon, E. I.; Brunold, T. C.; Davis, M. I.; Kemsley, J. N.; Lee, S. K.; Lehnert,
13 N.; Neese, F.; Skulan, A. J.; Yang, Y. S.; Zhou, J. Geometric and Electronic Structure/Function
14 Correlations in Non-Heme Iron Enzymes. *Chem. Rev.* **2000**, *100*, 235-349.
- 15 (3) Decker, A.; Solomon, E. I. Dioxygen Activation by Copper, Heme and Non-Heme
16 Iron Enzymes: Comparison of Electronic Structures and Reactivities. *Curr. Opin. Chem. Biol.*
17 **2005**, *9*, 152-163.
- 18 (4) Pau, M. Y. M.; Lipscomb, J. D.; Solomon, E. I. Substrate Activation for O₂
19 Reactions by Oxidized Metal Centers in Biology. *Proc. Natl. Acad. Sci. U.S.A.* **2007**, *104*, 18355-
20 18362.
- 21 (5) Groves, J. T. The Bioinorganic Chemistry of Iron in Oxygenases and
22 Supramolecular Assemblies. *Proc. Natl. Acad. Sci. U.S.A.* **2003**, *100*, 3569-3574.
- 23 (6) Drauz, K.; Gröger, H.; May, O. Introduction – Principles and Historical Landmarks
24 of Enzyme Catalysis in Organic Synthesis. In *Enzyme Catalysis in Organic Synthesis (Third*
25 *Edition)*; Wiley-VCH: Weinheim, Germany, 2012, p 1-42.
- 26 (7) Chen, K.; Arnold, F. H. Engineering New Catalytic Activities in Enzymes. *Nat.*
27 *Catal.* **2020**, *3*, 203-213.
- 28 (8) Munro, A. W.; Girvan, H. M.; McLean, K. J.; Cheesman, M. R.; Leys, D. Heme
29 and Hemoproteins. In *Tetrapyrroles: Birth, Life and Death*; Springer New York: New York, NY,
30 2009, p 160-183.
- 31 (9) Lash, T. D. Origin of Aromatic Character in Porphyrinoid Systems. *J. Porphyr.*
32 *Phthalocyanines* **2011**, *15*, 1093-1115.
- 33 (10) Dolphin, D.; Forman, A.; Borg, D. C.; Fajer, J.; Felton, R. H. Compounds I of
34 Catalase and Horse Radish Peroxidase: π -Cation Radicals. *Proc. Natl. Acad. Sci. U.S.A.* **1971**, *68*,
35 614-618.
- 36 (11) Dawson, J. Probing Structure-Function Relations in Heme-Containing Oxygenases
37 and Peroxidases. *Science* **1988**, *240*, 433-439.
- 38 (12) Hardison, R. C. A Brief History of Hemoglobins: Plant, Animal, Protist, and
39 Bacteria. *Proc. Natl. Acad. Sci. U.S.A.* **1996**, *93*, 5675-5679.
- 40 (13) Ordway, G. A.; Garry, D. J. Myoglobin: An Essential Hemoprotein in Striated
41 Muscle. *J. Exp. Biol.* **2004**, *207*, 3441-3446.
- 42 (14) Liu, J.; Chakraborty, S.; Hosseinzadeh, P.; Yu, Y.; Tian, S.; Petrik, I.; Bhagi, A.;
43 Lu, Y. Metalloproteins Containing Cytochrome, Iron–Sulfur, or Copper Redox Centers. *Chem.*
44 *Rev.* **2014**, *114*, 4366-4469.
- 45 (15) Chelikani, P.; Fita, I.; Loewen, P. C. Diversity of Structures and Properties Among
46 Catalases. *Cell. Mol. Life Sci.* **2004**, *61*, 192-208.
- 47 (16) Welinder, K. G. Superfamily of Plant, Fungal and Bacterial Peroxidases. *Curr.*
48 *Opin. Struct. Biol.* **1992**, *2*, 388-393.
49
50
51
52
53
54
55
56
57
58
59
60

- 1
2
3 (17) Alderton, W. K.; Cooper, C. E.; Knowles, R. G. Nitric Oxide Synthases: Structure,
4 Function and Inhibition. *Biochem. J.* **2001**, *357*, 593-615.
- 5 (18) Meunier, B.; de Visser, S. P.; Shaik, S. Mechanism of Oxidation Reactions
6 Catalyzed by Cytochrome P450 Enzymes. *Chem. Rev.* **2004**, *104*, 3947-3980.
- 7 (19) Huang, X.; Groves, J. T. Oxygen Activation and Radical Transformations in Heme
8 Proteins and Metalloporphyrins. *Chem. Rev.* **2018**, *118*, 2491-2553.
- 9 (20) Sono, M.; Roach, M. P.; Coulter, E. D.; Dawson, J. H. Heme-Containing
10 Oxygenases. *Chem. Rev.* **1996**, *96*, 2841-2888.
- 11 (21) Poulos, T. L. Heme Enzyme Structure and Function. *Chem. Rev.* **2014**, *114*, 3919-
12 3962.
- 13 (22) Baglia, R. A.; Zaragoza, J. P. T.; Goldberg, D. P. Biomimetic Reactivity of Oxygen-
14 Derived Manganese and Iron Porphyrinoid Complexes. *Chem. Rev.* **2017**, *117*, 13320-13352.
- 15 (23) Momenteau, M.; Reed, C. A. Synthetic Heme-Dioxygen Complexes. *Chem. Rev.*
16 **1994**, *94*, 659-698.
- 17 (24) Costas, M. Selective C–H oxidation catalyzed by metalloporphyrins. *Coord. Chem.*
18 *Rev.* **2011**, *255*, 2912-2932.
- 19 (25) Sahu, S.; Goldberg, D. P. Activation of Dioxygen by Iron and Manganese
20 Complexes: A Heme and Nonheme Perspective. *J. Am. Chem. Soc.* **2016**, *138*, 11410-11428.
- 21 (26) Fujii, H. Electronic Structure and Reactivity of High-Valent Oxo Iron Porphyrins.
22 *Coord. Chem. Rev.* **2002**, *226*, 51-60.
- 23 (27) Schlichting, I.; Berendzen, J.; Chu, K.; Stock, A. M.; Maves, S. A.; Benson, D. E.;
24 Sweet, R. M.; Ringe, D.; Petsko, G. A.; Sligar, S. G. The Catalytic Pathway of Cytochrome
25 P450cam at Atomic Resolution. *Science* **2000**, *287*, 1615-1622.
- 26 (28) de Visser, S. P.; Shaik, S. A Proton-Shuttle Mechanism Mediated by the Porphyrin
27 in Benzene Hydroxylation by Cytochrome P450 Enzymes. *J. Am. Chem. Soc.* **2003**, *125*, 7413-
28 7424.
- 29 (29) Newcomb, M.; Toy, P. H. Hypersensitive Radical Probes and the Mechanisms of
30 Cytochrome P450-Catalyzed Hydroxylation Reactions. *Acc. Chem. Res.* **2000**, *33*, 449-455.
- 31 (30) Seto, Y.; Guengerich, F. P. Partitioning Between *N*-Dealkylation and *N*-
32 Oxygenation in the Oxidation of *N,N*-Dialkylarylamines Catalyzed by Cytochrome P450 2B1. *J.*
33 *Biol. Chem.* **1993**, *268*, 9986-9997.
- 34 (31) Goto, Y.; Matsui, T.; Ozaki, S.-i.; Watanabe, Y.; Fukuzumi, S. Mechanisms of
35 Sulfoxidation Catalyzed by High-Valent Intermediates of Heme Enzymes: Electron-Transfer vs
36 Oxygen-Transfer Mechanism. *J. Am. Chem. Soc.* **1999**, *121*, 9497-9502.
- 37 (32) Anzai, Y.; Li, S.; Chaulagain, M. R.; Kinoshita, K.; Kato, F.; Montgomery, J.;
38 Sherman, D. H. Functional Analysis of MycCI and MycG, Cytochrome P450 Enzymes Involved
39 in Biosynthesis of Mycinamicin Macrolide Antibiotics. *Chem. Biol.* **2008**, *15*, 950-959.
- 40 (33) Rettie, A.; Rettenmeier, A.; Howald, W.; Baillie, T. Cytochrome P-450—Catalyzed
41 Formation of Δ^4 -VPA, a Toxic Metabolite of Valproic Acid. *Science* **1987**, *235*, 890-893.
- 42 (34) Kramlinger, V. M.; Nagy, L. D.; Fujiwara, R.; Johnson, K. M.; Phan, T. T. N.;
43 Xiao, Y.; Enright, J. M.; Toomey, M. B.; Corbo, J. C.; Guengerich, F. P. Human Cytochrome P450
44 27C1 Catalyzes 3,4-Desaturation of Retinoids. *FEBS Lett.* **2016**, *590*, 1304-1312.
- 45 (35) Belin, P.; Le Du, M. H.; Fielding, A.; Lequin, O.; Jacquet, M.; Charbonnier, J.-B.;
46 Lecoq, A.; Thai, R.; Courçon, M.; Masson, C.; Dugave, C.; Genet, R.; Pernodet, J.-L.; Gondry, M.
47 Identification and Structural Basis of the Reaction Catalyzed by CYP121, an Essential Cytochrome
48 P450 in *Mycobacterium tuberculosis*. *Proc. Natl. Acad. Sci. U.S.A.* **2009**, *106*, 7426-7431.
- 49
50
51
52
53
54
55
56
57

- 1
2
3 (36) Omura, T.; Sato, R. The Carbon Monoxide-Binding Pigment of Liver Microsomes:
4 I. Evidence for its Hemoprotein Nature. *J. Biol. Chem.* **1964**, *239*, 2370-2378.
5 (37) Nelson, D. R. The Cytochrome P450 Homepage. *Hum. Genet.* **2009**, *4*, 59.
6 (38) Chen, M. M.; Coelho, P. S.; Arnold, F. H. Utilizing Terminal Oxidants to Achieve
7 P450-Catalyzed Oxidation of Methane. *Adv. Synth. Catal.* **2012**, *354*, 964-968.
8 (39) Vallee, B. L.; Williams, R. J. Metalloenzymes: The Entatic Nature of Their Active
9 Sites. *Proc. Natl. Acad. Sci. U.S.A.* **1968**, *59*, 498-505.
10 (40) Sevrioukova, I. F.; Li, H.; Zhang, H.; Peterson, J. A.; Poulos, T. L. Structure of a
11 Cytochrome P450-Redox Partner Electron-Transfer Complex. *Proc. Natl. Acad. Sci. U.S.A.* **1999**,
12 *96*, 1863-1868.
13 (41) Sevrioukova, I.; Shaffer, C.; Ballou, D. P.; Peterson, J. A. Equilibrium and
14 Transient State Spectrophotometric Studies of the Mechanism of Reduction of the Flavoprotein
15 Domain of P450BM-3. *Biochemistry* **1996**, *35*, 7058-7068.
16 (42) Daff, S. N.; Chapman, S. K.; Holt, R. A.; Govindaraj, S.; Poulos, T. L.; Munro, A.
17 W. Redox Control of the Catalytic Cycle of Flavocytochrome P-450 BM3. *Biochemistry* **1997**, *36*,
18 13816-13823.
19 (43) Hlavica, P. Control by Substrate of the Cytochrome P450-Dependent Redox
20 Machinery: Mechanistic Insights. *Curr. Drug Metab.* **2007**, *8*, 594-611.
21 (44) Zangar, R. C.; Davydov, D. R.; Verma, S. Mechanisms That Regulate Production
22 of Reactive Oxygen Species by Cytochrome P450. *Toxicol. Appl. Pharmacol.* **2004**, *199*, 316-331.
23 (45) Baek, H. K.; Van Wart, H. E. Elementary Steps in the Formation of Horseradish
24 Peroxidase Compound I: Direct Observation of Compound 0, a New Intermediate with a
25 Hyperporphyrin Spectrum. *Biochemistry* **1989**, *28*, 5714-5719.
26 (46) Waskell, L.; Kim, J.-J. P. Electron Transfer Partners of Cytochrome P450. In
27 *Cytochrome P450*; Springer, Cham: Switzerland, 2015, p 33-68.
28 (47) Su, M.; Chakraborty, S.; Osawa, Y.; Zhang, H. Cryo-EM Reveals the Architecture
29 of the Dimeric Cytochrome P450 CYP102A1 Enzyme and Conformational Changes Required for
30 Redox Partner Recognition. *J. Biol. Chem.* **2020**, *295*, 1637-1645.
31 (48) Yeom, H.; Sligar, S. G.; Li, H.; Poulos, T. L.; Fulco, A. J. The Role of Thr268 in
32 Oxygen Activation of Cytochrome P450BM-3. *Biochemistry* **1995**, *34*, 14733-14740.
33 (49) Raag, R.; Martinis, S. A.; Sligar, S. G.; Poulos, T. L. Crystal Structure of the
34 Cytochrome P-450CAM Active Site Mutant Thr252Ala. *Biochemistry* **1991**, *30*, 11420-11429.
35 (50) Li, H.; Poulos, T. L. Modeling Protein-Substrate Interactions in the Heme Domain
36 of Cytochrome P450BM-3. *Acta Crystallogr., Sect. D: Biol. Crystallogr.* **1995**, *51*, 21-32.
37 (51) Shoji, O.; Fujishiro, T.; Nishio, K.; Kano, Y.; Kimoto, H.; Chien, S.-C.; Onoda, H.;
38 Muramatsu, A.; Tanaka, S.; Hori, A.; Sugimoto, H.; Shiro, Y.; Watanabe, Y. A Substrate-Binding-
39 State Mimic of H₂O₂-Dependent Cytochrome P450 Produced by One-Point Mutagenesis and
40 Peroxygenation of Non-Native Substrates. *Catal. Sci. Technol.* **2016**, *6*, 5806-5811.
41 (52) Dawson, J. H.; Sono, M. Cytochrome P-450 and Chloroperoxidase: Thiolate-
42 Ligated Heme Enzymes. Spectroscopic Determination of Their Active-Site Structures and
43 Mechanistic Implications of Thiolate Ligation. *Chem. Rev.* **1987**, *87*, 1255-1276.
44 (53) Green, M. T. Evidence for Sulfur-Based Radicals in Thiolate Compound I
45 Intermediates. *J. Am. Chem. Soc.* **1999**, *121*, 7939-7940.
46 (54) Yosca, T. H.; Rittle, J.; Krest, C. M.; Onderko, E. L.; Silakov, A.; Calixto, J. C.;
47 Behan, R. K.; Green, M. T. Iron(IV)hydroxide pK_a and the Role of Thiolate Ligation in C-H Bond
48 Activation by Cytochrome P450. *Science* **2013**, *342*, 825.
49
50
51
52
53
54
55
56
57
58
59
60

(55) Groves, J. T. Key Elements of the Chemistry of Cytochrome P-450: The Oxygen Rebound Mechanism. *J. Chem. Educ.* **1985**, *62*, 928-931.

(56) Green, M. T.; Dawson, J. H.; Gray, H. B. Oxoiron(IV) in Chloroperoxidase Compound II is Basic: Implications for P450 Chemistry. *Science* **2004**, *304*, 1653-1656.

(57) Green, M. T. C-H Bond Activation in Heme Proteins: The Role of Thiolate Ligation in Cytochrome P450. *Curr. Opin. Chem. Biol.* **2009**, *13*, 84-88.

(58) Krest, C. M.; Silakov, A.; Rittle, J.; Yosca, T. H.; Onderko, E. L.; Calixto, J. C.; Green, M. T. Significantly Shorter Fe-S Bond in Cytochrome P450-I is Consistent with Greater Reactivity Relative to Chloroperoxidase. *Nat. Chem.* **2015**, *7*, 696-702.

(59) Onderko, E. L.; Silakov, A.; Yosca, T. H.; Green, M. T. Characterization of a Selenocysteine-Ligated P450 Compound I Reveals Direct Link Between Electron Donation and Reactivity. *Nat. Chem.* **2017**, *9*, 623-628.

(60) Basran, J.; Booth, E. S.; Lee, M.; Handa, S.; Raven, E. L. Analysis of Reaction Intermediates in Tryptophan 2,3-Dioxygenase: A Comparison with Indoleamine 2,3-Dioxygenase. *Biochemistry* **2016**, *55*, 6743-6750.

(61) Geng, J.; Weitz, A. C.; Dornevil, K.; Hendrich, M. P.; Liu, A. Kinetic and Spectroscopic Characterization of the Catalytic Ternary Complex of Tryptophan 2,3-Dioxygenase. *Biochemistry* **2020**, *59*, 2813-2822.

(62) Davies, H. M. L.; Manning, J. R. Catalytic C-H Functionalization by Metal Carbenoid and Nitrenoid Insertion. *Nature* **2008**, *451*, 417-424.

(63) Hoffmann, R. Building Bridges Between Inorganic and Organic Chemistry (Nobel Lecture). *Angew. Chem. Int. Ed.* **1982**, *21*, 711-724.

(64) Coelho, P. S.; Brustad, E. M.; Kannan, A.; Arnold, F. H. Olefin Cyclopropanation via Carbene Transfer Catalyzed by Engineered Cytochrome P450 Enzymes. *Science* **2013**, *339*, 307-310.

(65) Coelho, P. S.; Wang, Z. J.; Ener, M. E.; Baril, S. A.; Kannan, A.; Arnold, F. H.; Brustad, E. M. A Serine-Substituted P450 Catalyzes Highly Efficient Carbene Transfer to Olefins *in vivo*. *Nat. Chem. Biol.* **2013**, *9*, 485-487.

(66) Knight, A. M.; Kan, S. B. J.; Lewis, R. D.; Brandenburg, O. F.; Chen, K.; Arnold, F. H. Diverse Engineered Heme Proteins Enable Stereodivergent Cyclopropanation of Unactivated Alkenes. *ACS Cent. Sci.* **2018**, *4*, 372-377.

(67) Brandenburg, O. F.; Prier, C. K.; Chen, K.; Knight, A. M.; Wu, Z.; Arnold, F. H. Stereoselective Enzymatic Synthesis of Heteroatom-Substituted Cyclopropanes. *ACS Catal.* **2018**, *8*, 2629-2634.

(68) Chen, K.; Zhang, S.-Q.; Brandenburg, O. F.; Hong, X.; Arnold, F. H. Alternate Heme Ligation Steers Activity and Selectivity in Engineered Cytochrome P450-Catalyzed Carbene-Transfer Reactions. *J. Am. Chem. Soc.* **2018**, *140*, 16402-16407.

(69) Brandenburg, O. F.; Chen, K.; Arnold, F. H. Directed Evolution of a Cytochrome P450 Carbene Transferase for Selective Functionalization of Cyclic Compounds. *J. Am. Chem. Soc.* **2019**, *141*, 8989-8995.

(70) Bordeaux, M.; Tyagi, V.; Fasan, R. Highly Diastereoselective and Enantioselective Olefin Cyclopropanation Using Engineered Myoglobin-Based Catalysts. *Angew. Chem. Int. Ed.* **2015**, *54*, 1744-1748.

(71) Tinoco, A.; Steck, V.; Tyagi, V.; Fasan, R. Highly Diastereo- and Enantioselective Synthesis of Trifluoromethyl-Substituted Cyclopropanes via Myoglobin-Catalyzed Transfer of Trifluoromethylcarbene. *J. Am. Chem. Soc.* **2017**, *139*, 5293-5296.

(72) Chandgude, A. L.; Fasan, R. Highly Diastereo- and Enantioselective Synthesis of Nitrile-Substituted Cyclopropanes by Myoglobin-Mediated Carbene Transfer Catalysis. *Angew. Chem. Int. Ed.* **2018**, *57*, 15852-15856.

(73) Chandgude, A. L.; Ren, X.; Fasan, R. Stereodivergent Intramolecular Cyclopropanation Enabled by Engineered Carbene Transferases. *J. Am. Chem. Soc.* **2019**, *141*, 9145-9150.

(74) Vargas, D. A.; Khade, R. L.; Zhang, Y.; Fasan, R. Biocatalytic Strategy for Highly Diastereo- and Enantioselective Synthesis of 2,3-Dihydrobenzofuran-Based Tricyclic Scaffolds. *Angew. Chem. Int. Ed.* **2019**, *58*, 10148-10152.

(75) Carminati, D. M.; Fasan, R. Stereoselective Cyclopropanation of Electron-Deficient Olefins with a Cofactor Redesign Carbene Transferase Featuring Radical Reactivity. *ACS Catal.* **2019**, *9*, 9683-9697.

(76) Ren, X.; Chandgude, A. L.; Fasan, R. Highly Stereoselective Synthesis of Fused Cyclopropane- γ -Lactams via Biocatalytic Iron-Catalyzed Intramolecular Cyclopropanation. *ACS Catal.* **2020**, *10*, 2308-2313.

(77) Renata, H.; Wang, Z. J.; Kitto, R. Z.; Arnold, F. H. P450-Catalyzed Asymmetric Cyclopropanation of Electron-Deficient Olefins Under Aerobic Conditions. *Catal. Sci. Technol.* **2014**, *4*, 3640-3643.

(78) Wittmann, B. J.; Knight, A. M.; Hofstra, J. L.; Reisman, S. E.; Jennifer Kan, S. B.; Arnold, F. H. Diversity-Oriented Enzymatic Synthesis of Cyclopropane Building Blocks. *ACS Catal.* **2020**, *10*, 7112-7116.

(79) Chen, K.; Huang, X.; Kan, S. B. J.; Zhang, R. K.; Arnold, F. H. Enzymatic Construction of Highly Strained Carbocycles. *Science* **2018**, *360*, 71-75.

(80) Chen, K.; Arnold, F. H. Engineering Cytochrome P450s for Enantioselective Cyclopropanation of Internal Alkynes. *J. Am. Chem. Soc.* **2020**, *142*, 6891-6895.

(81) Wang, Z. J.; Peck, N. E.; Renata, H.; Arnold, F. H. Cytochrome P450-Catalyzed Insertion of Carbenoids into N-H Bonds. *Chem. Sci.* **2014**, *5*, 598-601.

(82) Sreenilayam, G.; Fasan, R. Myoglobin-Catalyzed Intermolecular Carbene N-H Insertion with Arylamine Substrates. *ChemComm* **2015**, *51*, 1532-1534.

(83) Tyagi, V.; Bonn, R. B.; Fasan, R. Intermolecular Carbene S-H Insertion Catalysed by Engineered Myoglobin-Based Catalysts. *Chem. Sci.* **2015**, *6*, 2488-2494.

(84) Kan, S. B. J.; Lewis, R. D.; Chen, K.; Arnold, F. H. Directed Evolution of Cytochrome *c* for Carbon-Silicon Bond Formation: Bringing Silicon to Life. *Science* **2016**, *354*, 1048-1051.

(85) Kan, S. B. J.; Huang, X. Y.; Gumulya, Y.; Chen, K.; Arnold, F. H. Genetically Programmed Chiral Organoborane Synthesis. *Nature* **2017**, *552*, 132-+.

(86) Chen, K.; Huang, X.; Zhang, S.-Q.; Zhou, A. Z.; Kan, S. B. J.; Hong, X.; Arnold, F. H. Engineered Cytochrome *c*-Catalyzed Lactone-Carbene B-H Insertion. *Synlett* **2019**, *30*, 378-382.

(87) Huang, X.; Garcia-Borràs, M.; Miao, K.; Kan, S. B. J.; Zutshi, A.; Houk, K. N.; Arnold, F. H. A Biocatalytic Platform for Synthesis of Chiral α -Trifluoromethylated Organoborons. *ACS Cent. Sci.* **2019**, *5*, 270-276.

(88) Zhang, R. K.; Chen, K.; Huang, X.; Wohlschlager, L.; Renata, H.; Arnold, F. H. Enzymatic Assembly of Carbon-Carbon Bonds via Iron-Catalysed sp^3 C-H Functionalization. *Nature* **2019**, *565*, 67-72.

- (89) Zhang, J.; Huang, X.; Zhang, R. K.; Arnold, F. H. Enantiodivergent α -Amino C–H Fluoroalkylation Catalyzed by Engineered Cytochrome P450s. *J. Am. Chem. Soc.* **2019**, *141*, 9798-9802.
- (90) Zhou, A. Z.; Chen, K.; Arnold, F. H. Enzymatic Lactone-Carbene C–H Insertion to Build Contiguous Chiral Centers. *ACS Catal.* **2020**, *10*, 5393-5398.
- (91) Svastits, E. W.; Dawson, J. H.; Breslow, R.; Gellman, S. H. Functionalized Nitrogen Atom Transfer Catalyzed by Cytochrome P-450. *J. Am. Chem. Soc.* **1985**, *107*, 6427-6428.
- (92) McIntosh, J. A.; Coelho, P. S.; Farwell, C. C.; Wang, Z. J.; Lewis, J. C.; Brown, T. R.; Arnold, F. H. Enantioselective Intramolecular C-H Amination Catalyzed by Engineered Cytochrome P450 Enzymes In Vitro and In Vivo. *Angew. Chem. Int. Ed.* **2013**, *52*, 9309-9312.
- (93) Singh, R.; Bordeaux, M.; Fasan, R. P450-Catalyzed Intramolecular sp^3 C–H Amination with Arylsulfonyl Azide Substrates. *ACS Catal.* **2014**, *4*, 546-552.
- (94) Prier, C. K.; Zhang, R. J. K.; Buller, A. R.; Brinkmann-Chen, S.; Arnold, F. H. Enantioselective, Intermolecular Benzylic C-H Amination Catalysed by an Engineered Iron-haem Enzyme. *Nat. Chem.* **2017**, *9*, 629-634.
- (95) Farwell, C. C.; Zhang, R. K.; McIntosh, J. A.; Hyster, T. K.; Arnold, F. H. Enantioselective Enzyme-Catalyzed Aziridination Enabled by Active-Site Evolution of a Cytochrome P450. *ACS Cent. Sci.* **2015**, *1*, 89-93.
- (96) Sabir, S.; Kumar, G.; Jat, J. L. *O*-Substituted Hydroxyl Amine Reagents: An Overview of Recent Synthetic Advances. *Org. Biomol. Chem.* **2018**, *16*, 3314-3327.
- (97) Tsutsumi, H.; Katsuyama, Y.; Izumikawa, M.; Takagi, M.; Fujie, M.; Satoh, N.; Shin-ya, K.; Ohnishi, Y. Unprecedented Cyclization Catalyzed by a Cytochrome P450 in Benzastatin Biosynthesis. *J. Am. Chem. Soc.* **2018**, *140*, 6631-6639.
- (98) Cho, I.; Prier, C. K.; Jia, Z.-J.; Zhang, R. K.; Görbe, T.; Arnold, F. H. Enantioselective Aminohydroxylation of Styrenyl Olefins Catalyzed by an Engineered Hemoprotein. *Angew. Chem. Int. Ed.* **2019**, *58*, 3138-3142.
- (99) Jia, Z.-J.; Gao, S.; Arnold, F. H. Enzymatic Primary Amination of Benzylic and Allylic C(sp³)–H Bonds. *J. Am. Chem. Soc.* **2020**, *142*, 10279-10283.
- (100) Moore, E. J.; Fasan, R. Effect of Proximal Ligand Substitutions on the Carbene and Nitrene Transferase Activity of Myoglobin. *Tetrahedron* **2019**, *75*, 2357-2363.
- (101) Green, A. P.; Hayashi, T.; Mittl, P. R. E.; Hilvert, D. A Chemically Programmed Proximal Ligand Enhances the Catalytic Properties of a Heme Enzyme. *J. Am. Chem. Soc.* **2016**, *138*, 11344-11352.
- (102) Pott, M.; Hayashi, T.; Mori, T.; Mittl, P. R. E.; Green, A. P.; Hilvert, D. A Noncanonical Proximal Heme Ligand Affords an Efficient Peroxidase in a Globin Fold. *J. Am. Chem. Soc.* **2018**, *140*, 1535-1543.
- (103) Renata, H.; Lewis, R. D.; Sweredoski, M. J.; Moradian, A.; Hess, S.; Wang, Z. J.; Arnold, F. H. Identification of Mechanism-Based Inactivation in P450-Catalyzed Cyclopropanation Facilitates Engineering of Improved Enzymes. *J. Am. Chem. Soc.* **2016**, *138*, 12527-12533.
- (104) Farwell, C. C.; McIntosh, J. A.; Hyster, T. K.; Wang, Z. J.; Arnold, F. H. Enantioselective Imidation of Sulfides via Enzyme-Catalyzed Intermolecular Nitrogen-Atom Transfer. *J. Am. Chem. Soc.* **2014**, *136*, 8766-8771.
- (105) Fenton, H. J. H. LXXIII.—Oxidation of Tartaric Acid in Presence of Iron. *J. Chem. Soc., Trans.* **1894**, *65*, 899-910.

- 1
2
3 (106) Bryant, J. D.; Wilson, J. T. Fenton's *in-situ* Reagent Chemical Oxidation of
4 Hydrocarbon Contamination in Soil and Groundwater. *Remediation* **1999**, *9*, 13-25.
- 5 (107) Groves, J. T.; Van der Puy, M. Stereospecific Aliphatic Hydroxylation by Iron-
6 Hydrogen Peroxide. Evidence for a Stepwise Process. *J. Am. Chem. Soc.* **1976**, *98*, 5290-5297.
- 7 (108) Groves, J. T. High-Valent Iron in Chemical and Biological Oxidations. *J. Inorg.*
8 *Biochem.* **2006**, *100*, 434-447.
- 9 (109) Loegager, T.; Holcman, J.; Sehested, K.; Pedersen, T. Oxidation of Ferrous Ions by
10 Ozone in Acidic Solutions. *Inorg. Chem.* **1992**, *31*, 3523-3529.
- 11 (110) Pestovsky, O.; Bakac, A. Reactivity of Aqueous Fe(IV) in Hydride and Hydrogen
12 Atom Transfer Reactions. *J. Am. Chem. Soc.* **2004**, *126*, 13757-13764.
- 13 (111) Barton, D. H. R.; Gastiger, M. J.; Motherwell, W. B. A New Procedure for the
14 Oxidation of Saturated Hydrocarbons. *J. Chem. Soc., Chem. Commun.* **1983**, 41-43.
- 15 (112) Barton, D. H. R.; Doller, D. The Selective Functionalization of Saturated
16 Hydrocarbons: Gif Chemistry. *Acc. Chem. Res.* **1992**, *25*, 504-512.
- 17 (113) Stavropoulos, P.; Çelenligil-Çetin, R.; Tapper, A. E. The Gif Paradox. *Acc. Chem.*
18 *Res.* **2001**, *34*, 745-752.
- 19 (114) Hegg, E. L.; Jr, L. Q. The 2-His-1-Carboxylate Facial Triad — An Emerging
20 Structural Motif in Mononuclear Non-Heme Iron(II) Enzymes. *Eur. J. Biochem.* **1997**, *250*, 625-
21 629.
- 22 (115) Koehntop, K. D.; Emerson, J. P.; Que, L., Jr. The 2-His-1-Carboxylate Facial Triad:
23 A Versatile Platform for Dioxygen Activation by Mononuclear Non-Heme Iron(II) Enzymes. *J.*
24 *Biol. Inorg. Chem.* **2005**, *10*, 87-93.
- 25 (116) Kal, S.; Que, L. Dioxygen Activation by Nonheme Iron Enzymes with the 2-His-
26 1-Carboxylate Facial Triad That Generate High-Valent Oxoiron Oxidants. *J. Biol. Inorg. Chem.*
27 **2017**, *22*, 339-365.
- 28 (117) Lipscomb, J. D. Mechanism of Extradial Aromatic Ring-Cleaving Dioxygenases.
29 *Curr. Opin. Struct. Biol.* **2008**, *18*, 644-649.
- 30 (118) Barry, S. M.; Challis, G. L. Mechanism and Catalytic Diversity of Rieske Non-
31 Heme Iron-Dependent Oxygenases. *ACS Catal.* **2013**, *3*, 2362-2370.
- 32 (119) Martinez, S.; Hausinger, R. P. Catalytic Mechanisms of Fe(II)- and 2-Oxoglutarate-
33 dependent Oxygenases. *J. Biol. Chem.* **2015**, *290*, 20702-20711.
- 34 (120) Fitzpatrick, P. F. Mechanism of Aromatic Amino Acid Hydroxylation.
35 *Biochemistry* **2003**, *42*, 14083-14091.
- 36 (121) Baldwin, J. E.; Bradley, M. Isopenicillin N Synthase: Mechanistic Studies. *Chem.*
37 *Rev.* **1990**, *90*, 1079-1088.
- 38 (122) Tamanaha, E.; Zhang, B.; Guo, Y.; Chang, W. C.; Barr, E. W.; Xing, G.; St Clair,
39 J.; Ye, S.; Neese, F.; Bollinger, J. M., Jr.; Krebs, C. Spectroscopic Evidence for the Two C-H-
40 Cleaving Intermediates of *Aspergillus nidulans* Isopenicillin N Synthase. *J. Am. Chem. Soc.* **2016**,
41 *138*, 8862-8874.
- 42 (123) Wang, C.; Chang, W. C.; Guo, Y. S.; Huang, H.; Peck, S. C.; Pandelia, M. E.; Lin,
43 G. M.; Liu, H. W.; Krebs, C.; Bollinger, J. M. Evidence that the Fosfomycin-Producing Epoxidase,
44 HppE, is a Non-Heme-Iron Peroxidase. *Science* **2013**, *342*, 991-995.
- 45 (124) Peck, S. C.; Wang, C.; Dassama, L. M. K.; Zhang, B.; Guo, Y.; Rajakovich, L. J.;
46 Bollinger, J. M.; Krebs, C.; van der Donk, W. A. O-H Activation by an Unexpected Ferryl
47 Intermediate during Catalysis by 2-Hydroxyethylphosphonate Dioxygenase. *J. Am. Chem. Soc.*
48 **2017**, *139*, 2045-2052.
- 49
50
51
52
53
54
55
56
57
58
59
60

(125) Born, D. A.; Ulrich, E. C.; Ju, K.-S.; Peck, S. C.; van der Donk, W. A.; Drennan, C. L. Structural Basis for Methylphosphonate Biosynthesis. *Science* **2017**, *358*, 1336-1339.

(126) Mirica, L. M.; Klinman, J. P. The Nature of O₂ Activation by the Ethylene-Forming Enzyme 1-Aminocyclopropane-1-Carboxylic Acid Oxidase. *Proc. Natl. Acad. Sci. U.S.A.* **2008**, *105*, 1814-1819.

(127) Puri, M.; Que, L. Toward the Synthesis of More Reactive $S = 2$ Non-Heme Oxoiron(IV) Complexes. *Acc. Chem. Res.* **2015**, *48*, 2443-2452.

(128) Oloo, W. N.; Que, L. Bioinspired Nonheme Iron Catalysts for C–H and C=C Bond Oxidation: Insights into the Nature of the Metal-Based Oxidants. *Acc. Chem. Res.* **2015**, *48*, 2612-2621.

(129) Kal, S.; Xu, S.; Que Jr., L. Bio-inspired Nonheme Iron Oxidation Catalysis: Involvement of Oxoiron(V) Oxidants in Cleaving Strong C–H Bonds. *Angew. Chem. Int. Ed.* **2020**, *59*, 7332-7349.

(130) Roach, R. L.; Clifton, I. J.; Hensgens, C. M. H.; Shibata, N.; Schofield, C. J.; Hajdu, J.; Baldwin, J. E. Structure of Isopenicillin *N* Synthase Complexed with Substrate and the Mechanism of Penicillin Formation. *Nature* **1997**, *387*.

(131) Zhang, Z.; Ren, J.-s.; Harlos, K.; McKinnon, C. H.; Clifton, I. J.; Schofield, C. J. Crystal Structure of a Clavamate Synthase-Fe(II)-2-Oxoglutarate-Substrate-NO Complex: Evidence for Metal Centered Rearrangements. *FEBS Lett.* **2002**, *517*, 7-12.

(132) Mitchell, A. J.; Zhu, Q.; Maggiolo, A. O.; Ananth, N. R.; Hillwig, M. L.; Liu, X.; Boal, A. K. Structural Basis for Halogenation by Iron- and 2-Oxo-Glutarate-Dependent Enzyme WelO5. *Nat. Chem. Biol.* **2016**, *12*, 636-640.

(133) Bassan, A.; Blomberg, M. R. A.; Siegbahn, P. E. M. Mechanism of Dioxygen Cleavage in Tetrahydrobiopterin-Dependent Amino Acid Hydroxylases. *Chem. Eur. J.* **2003**, *9*, 106-115.

(134) Olsson, E.; Martinez, A.; Teigen, K.; Jensen, V. R. Formation of the Iron–Oxo Hydroxylating Species in the Catalytic Cycle of Aromatic Amino Acid Hydroxylases. *Chem. Eur. J.* **2011**, *17*, 3746-3758.

(135) Andreas Andersen, O.; Flatmark, T.; Hough, E. Crystal Structure of the Ternary Complex of the Catalytic Domain of Human Phenylalanine Hydroxylase with Tetrahydrobiopterin and 3-(2-Thienyl)-l-alanine, and its Implications for the Mechanism of Catalysis and Substrate Activation. *J. Mol. Biol.* **2002**, *320*, 1095-1108.

(136) Karlsson, A.; Parales, J. V.; Parales, R. E.; Gibson, D. T.; Eklund, H.; Ramaswamy, S. Crystal Structure of Naphthalene Dioxygenase: Side-on Binding of Dioxygen to Iron. *Science* **2003**, *299*, 1039-1042.

(137) Ashikawa, Y.; Fujimoto, Z.; Usami, Y.; Inoue, K.; Noguchi, H.; Yamane, H.; Nojiri, H. Structural Insight Into the Substrate- and Dioxygen-Binding Manner in the Catalytic Cycle of Rieske Nonheme Iron Oxygenase System, Carbazole 1,9a-Dioxygenase. *BMC Struct. Biol.* **2012**, *12*, 15.

(138) Kovaleva, E. G.; Lipscomb, J. D. Crystal Structures of Fe(II) Dioxygenase Superoxo, Alkylperoxo, and Bound Product Intermediates. *Science* **2007**, *316*, 453-457.

(139) Wang, Y.; Liu, K. F.; Yang, Y.; Davis, I.; Liu, A. Observing 3-Hydroxyanthranilate-3,4-Dioxygenase in Action Through a Crystalline Lens. *Proc. Natl. Acad. Sci. U.S.A.* **2020**, *117*, 19720-19730.

(140) Krebs, C.; Galonić Fujimori, D.; Walsh, C. T.; Bollinger, J. M., Jr. Non-Heme Fe(IV)-Oxo Intermediates. *Acc. Chem. Res.* **2007**, *40*, 484-493.

(141) Herr, C. Q.; Hausinger, R. P. Amazing Diversity in Biochemical Roles of Fe(II)/2-Oxoglutarate Oxygenases. *Trends Biochem. Sci.* **2018**, *43*, 517-532.

(142) Price, J. C.; Barr, E. W.; Tirupati, B.; Bollinger, J. M., Jr.; Krebs, C. The First Direct Characterization of a High-Valent Iron Intermediate in the Reaction of an α -Ketoglutarate-Dependent Dioxygenase: A High-Spin Fe(IV) Complex in Taurine/ α -Ketoglutarate Dioxygenase (TauD) from *Escherichia coli*. *Biochemistry* **2003**, *42*, 7497-7508.

(143) Price, J. C.; Barr, E. W.; Glass, T. E.; Krebs, C.; Bollinger, J. M., Jr. Evidence for Hydrogen Abstraction from C1 of Taurine by the High-Spin Fe(IV) Intermediate Detected During Oxygen Activation by Taurine: α -Ketoglutarate Dioxygenase (TauD). *J. Am. Chem. Soc.* **2003**, *125*, 13008-13009.

(144) Hoffart, L. M.; Barr, E. W.; Guyer, R. B.; Bollinger, J. M., Jr.; Krebs, C. Direct Spectroscopic Detection of a C-H-Cleaving High-Spin Fe(IV) Complex in a Prolyl-4-Hydroxylase. *Proc. Natl. Acad. Sci. U.S.A.* **2006**, *103*, 14738-14743.

(145) Galonić, D. P.; Barr, E. W.; Walsh, C. T.; Bollinger, J. M., Jr.; Krebs, C. Two Interconverting Fe(IV) Intermediates in Aliphatic Chlorination by the Halogenase CytC3. *Nat. Chem. Biol.* **2007**, *3*, 113-116.

(146) Matthews, M. L.; Krest, C. M.; Barr, E. W.; Vaillancourt, F. H.; Walsh, C. T.; Green, M. T.; Krebs, C.; Bollinger, J. M., Jr. Substrate-Triggered Formation and Remarkable Stability of the C-H Bond-Cleaving Chloroferryl Intermediate in the Aliphatic Halogenase, SyrB2. *Biochemistry* **2009**, *48*, 4331-4343.

(147) Grzyska, P. K.; Appelman, E. H.; Hausinger, R. P.; Proshlyakov, D. A. Insight Into the Mechanism of an Iron Dioxygenase by Resolution of Steps Following the Fe(IV)=O Species. *Proc. Natl. Acad. Sci. U.S.A.* **2010**, *107*, 3982-3987.

(148) Chang, W.-c.; Guo, Y.; Wang, C.; Butch, S. E.; Rosenzweig, A. C.; Boal, A. K.; Krebs, C.; Bollinger, J. M., Jr. Mechanism of the C5 Stereoconversion Reaction in the Biosynthesis of Carbapenem Antibiotics. *Science* **2014**, *343*, 1140-1144.

(149) Mitchell, A. J.; Dunham, N. P.; Martinie, R. J.; Bergman, J. A.; Pollock, C. J.; Hu, K.; Allen, B. D.; Chang, W. C.; Silakov, A.; Bollinger, J. M., Jr.; Krebs, C.; Boal, A. K. Visualizing the Reaction Cycle in an Iron(II)- and 2-(Oxo)-glutarate-Dependent Hydroxylase. *J. Am. Chem. Soc.* **2017**, *139*, 13830-13836.

(150) Pan, J.; Bhardwaj, M.; Zhang, B.; Chang, W. c.; Schardl, C. L.; Krebs, C.; Grossman, R. B.; Bollinger, J. M., Jr. Installation of the Ether Bridge of Lolines by the Iron- and 2-Oxoglutarate-Dependent Oxygenase, LolO: Regio- and Stereochemistry of Sequential Hydroxylation and Oxacyclization Reactions. *Biochemistry* **2018**, *57*, 2074-2083.

(151) Pan, J.; Wenger, E. S.; Matthews, M. L.; Pollock, C. J.; Bhardwaj, M.; Kim, A. J.; Allen, B. D.; Grossman, R. B.; Krebs, C.; Bollinger, J. M. Evidence for Modulation of Oxygen Rebound Rate in Control of Outcome by Iron(II)- and 2-Oxoglutarate-Dependent Oxygenases. *J. Am. Chem. Soc.* **2019**, *141*, 15153-15165.

(152) Li, J.; Liao, H.-J.; Tang, Y.; Huang, J.-L.; Cha, L.; Lin, T.-S.; Lee, J. L.; Kurnikov, I. V.; Kurnikova, M. G.; Chang, W.-c.; Chan, N.-L.; Guo, Y. Epoxidation Catalyzed by the Nonheme Iron(II)- and 2-Oxoglutarate-Dependent Oxygenase, AsqJ: Mechanistic Elucidation of Oxygen Atom Transfer by a Ferryl Intermediate. *J. Am. Chem. Soc.* **2020**, *142*, 6268-6284.

(153) Blasiak, L. C.; Vaillancourt, F. H.; Walsh, C. T.; Drennan, C. L. Crystal Structure of the Non-Haem Iron Halogenase SyrB2 in Syringomycin Biosynthesis. *Nature* **2006**, *440*, 368-371.

1
2
3 (154) Matthews, M. L.; Neumann, C. S.; Miles, L. A.; Grove, T. L.; Booker, S. J.; Krebs,
4 C.; Walsh, C. T.; Bollinger, J. M., Jr. Substrate Positioning Controls the Partition Between
5 Halogenation and Hydroxylation in the Aliphatic Halogenase, SyrB2. *Proc. Natl. Acad. Sci. U.S.A.*
6 **2009**, *106*, 17723-17728.

7
8 (155) Wong, S. D.; Srnec, M.; Matthews, M. L.; Liu, L. V.; Kwak, Y.; Park, K.; Bell, C.
9 B., 3rd; Alp, E. E.; Zhao, J.; Yoda, Y.; Kitao, S.; Seto, M.; Krebs, C.; Bollinger, J. M., Jr.; Solomon,
10 E. I. Elucidation of the Fe(IV)=O Intermediate in the Catalytic Cycle of the Halogenase SyrB2.
11 *Nature* **2013**, *499*, 320-323.

12 (156) Martinie, R. J.; Livada, J.; Chang, W.-c.; Green, M. T.; Krebs, C.; Bollinger, J. M.,
13 Jr.; Silakov, A. Experimental Correlation of Substrate Position with Reaction Outcome in the
14 Aliphatic Halogenase, SyrB2. *J. Am. Chem. Soc.* **2015**, *137*, 6912-6919.

15 (157) Dunham, N. P.; Chang, W.-c.; Mitchell, A. J.; Martinie, R. J.; Zhang, B.; Bergman,
16 J. A.; Rajakovich, L. J.; Wang, B.; Silakov, A.; Krebs, C.; Boal, A. K.; Bollinger, J. M., Jr. Two
17 Distinct Mechanisms for C-C Desaturation by Iron(II)- and 2-(Oxo)glutarate-Dependent
18 Oxygenases: Importance of Alpha-Heteroatom Assistance. *J. Am. Chem. Soc.* **2018**, *140*, 7116-
19 7126.

20 (158) Ushimaru, R.; Ruzsyczky, M. W.; Liu, H.-w. Changes in Regioselectivity of H
21 Atom Abstraction during the Hydroxylation and Cyclization Reactions Catalyzed by Hyoscyamine
22 6 β -Hydroxylase. *J. Am. Chem. Soc.* **2019**, *141*, 1062-1066.

23 (159) Chang, W.-c.; Yang, Z.-J.; Tu, Y.-H.; Chien, T.-C. Reaction Mechanism of a
24 Nonheme Iron Enzyme Catalyzed Oxidative Cyclization via C-C Bond Formation. *Org. Lett.*
25 **2019**, *21*, 228-232.

26 (160) Borowski, T.; de Marothy, S.; Broclawik, E.; Schofield, C. J.; Siegbahn, P. E. M.
27 Mechanism for Cyclization Reaction by Clavaminc Acid Synthase. Insights From Modeling
28 Studies. *Biochemistry* **2007**, *46*, 3682-3691.

29 (161) Dunham, N. P.; Del Río Pantoja, J. M.; Zhang, B.; Rajakovich, L. J.; Allen, B. D.;
30 Krebs, C.; Boal, A. K.; Bollinger, J. M. Hydrogen Donation but not Abstraction by a Tyrosine
31 (Y68) During Endoperoxide Installation by Verruculogen Synthase (FtmOx1). *J. Am. Chem. Soc.*
32 **2019**, *141*, 9964-9979.

33 (162) Liu, W.; Groves, J. T. Manganese Porphyrins Catalyze Selective C-H Bond
34 Halogenations. *J. Am. Chem. Soc.* **2010**, *132*, 12847-12849.

35 (163) Liu, W.; Huang, X.; Cheng, M.-J.; Nielsen, R. J.; Goddard, W. A.; Groves, J. T.
36 Oxidative Aliphatic C-H Fluorination with Fluoride Ion Catalyzed by a Manganese Porphyrin.
37 *Science* **2012**, *337*, 1322-1325.

38 (164) Schmidt, V. A.; Quinn, R. K.; Brusoe, A. T.; Alexanian, E. J. Site-Selective
39 Aliphatic C-H Bromination Using N-Bromoamides and Visible Light. *J. Am. Chem. Soc.* **2014**,
40 *136*, 14389-14392.

41 (165) Liu, W.; Groves, J. T. Manganese Catalyzed C-H Halogenation. *Acc. Chem. Res.*
42 **2015**, *48*, 1727-1735.

43 (166) Margrey, K. A.; Czaplyski, W. L.; Nicewicz, D. A.; Alexanian, E. J. A General
44 Strategy for Aliphatic C-H Functionalization Enabled by Organic Photoredox Catalysis. *J. Am.*
45 *Chem. Soc.* **2018**, *140*, 4213-4217.

46 (167) Matthews, M. L.; Chang, W. C.; Layne, A. P.; Miles, L. A.; Krebs, C.; Bollinger,
47 J. M., Jr. Direct Nitration and Azidation of Aliphatic Carbons by an Iron-Dependent Halogenase.
48 *Nat. Chem. Biol.* **2014**, *10*, 209-215.

- 1
2
3 (168) Neugebauer, M. E.; Sumida, K. H.; Pelton, J. G.; McMurry, J. L.; Marchand, J. A.;
4 Chang, M. C. Y. A family of Radical Halogenases for the Engineering of Amino-Acid-Based
5 Products. *Nat. Chem. Biol.* **2019**, *15*, 1009-1016.
- 6 (169) Kim, C. Y.; Mitchell, A. J.; Glinkerman, C. M.; Li, F.-S.; Pluskal, T.; Weng, J.-K.
7 The Chloroalkaloid (-)-Acutumine is Biosynthesized via a Fe(II)- and 2-Oxoglutarate-Dependent
8 Halogenase in *Menispermaceae* Plants. *Nat. Commun.* **2020**, *11*, 1867.
- 9 (170) Jewett, J. C.; Bertozzi, C. R. Cu-Free Click Cycloaddition Reactions in Chemical
10 Biology. *Chem. Soc. Rev.* **2010**, *39*, 1272-1279.
- 11 (171) Mitchell, A. J.; Dunham, N. P.; Bergman, J. A.; Wang, B.; Zhu, Q.; Chang, W.-c.;
12 Liu, X.; Boal, A. K. Structure-Guided Reprogramming of a Hydroxylase to Halogenate its Small
13 Molecule Substrate. *Biochemistry* **2017**, *56*, 441-444.
- 14 (172) Davidson, M.; McNamee, M.; Fan, R.; Guo, Y.; Chang, W.-c. Repurposing
15 Nonheme Iron Hydroxylases To Enable Catalytic Nitrile Installation through an Azido Group
16 Assistance. *J. Am. Chem. Soc.* **2019**, *141*, 3419-3423.
- 17 (173) Vila, M. A.; Pazos, M.; Iglesias, C.; Veiga, N.; Seoane, G.; Carrera, I. Toluene
18 Dioxygenase-Catalysed Oxidation of Benzyl Azide to Benzotrile: Mechanistic Insights for an
19 Unprecedented Enzymatic Transformation. *ChemBioChem* **2016**, *17*, 291-295.
- 20 (174) Goldberg, N. W.; Knight, A. M.; Zhang, R. K.; Arnold, F. H. Nitrene Transfer
21 Catalyzed by a Non-Heme Iron Enzyme and Enhanced by Non-Native Small-Molecule Ligands.
22 *J. Am. Chem. Soc.* **2019**, *141*, 19585-19588.
- 23 (175) Vila, M. A.; Steck, V.; Rodriguez Giordano, S.; Carrera, I.; Fasan, R. C-H
24 Amination via Nitrene Transfer Catalyzed by Mononuclear Non-Heme Iron-Dependent Enzymes.
25 *ChemBioChem* **2020**, *21*, 1981-1987.
- 26 (176) Hammer, S. C.; Knight, A. M.; Arnold, F. H. Design and Evolution of Enzymes for
27 Non-Natural Chemistry. *Curr. Opin. Green Sustain. Chem.* **2017**, *7*, 23-30.
- 28 (177) Reetz, M. T.; Carballeira, J. D. Iterative Saturation Mutagenesis (ISM) for Rapid
29 Directed Evolution of Functional Enzymes. *Nat. Protoc.* **2007**, *2*, 891-903.
- 30 (178) Renata, H.; Wang, Z. J.; Arnold, F. H. Expanding the Enzyme Universe: Accessing
31 Non-Natural Reactions by Mechanism-Guided Directed Evolution. *Angew. Chem. Int. Ed.* **2015**,
32 *54*, 3351-3367.
- 33 (179) Haines, D. C.; Tomchick, D. R.; Machius, M.; Peterson, J. A. Pivotal Role of Water
34 in the Mechanism of P450BM-3. *Biochemistry* **2001**, *40*, 13456-13465.
- 35 (180) Lewis, R. D.; Garcia-Borràs, M.; Chalkley, M. J.; Buller, A. R.; Houk, K. N.; Kan,
36 S. B. J.; Arnold, F. H. Catalytic Iron-Carbene Intermediate Revealed in a Cytochrome *c* Carbene
37 Transferase. *Proc. Natl. Acad. Sci. U.S.A.* **2018**, *115*, 7308-7313.
- 38 (181) Zhang, X.; Peng, Y.; Zhao, J.; Li, Q.; Yu, X.; Acevedo-Rocha, C. G.; Li, A.
39 Bacterial Cytochrome P450-Catalyzed Regio- and Stereoselective Steroid Hydroxylation Enabled
40 by Directed Evolution and Rational Design. *Bioresour. Bioprocess.* **2020**, *7*, 2.
- 41 (182) Li, R.-J.; Zhang, Z.; Acevedo-Rocha, C. G.; Zhao, J.; Li, A. Biosynthesis of
42 Organic Molecules via Artificial Cascade Reactions Based on Cytochrome P450
43 Monooxygenases. *Green Synth. Catal.* **2020**, *1*, 52-59.
- 44 (183) Loskot, S. A.; Romney, D. K.; Arnold, F. H.; Stoltz, B. M. Enantioselective Total
45 Synthesis of Nigelladine A via Late-Stage C-H Oxidation Enabled by an Engineered P450
46 Enzyme. *J. Am. Chem. Soc.* **2017**, *139*, 10196-10199.
- 47
48
49
50
51
52
53
54
55
56
57
58
59
60

(184) Li, J.; Li, F.; King-Smith, E.; Renata, H. Merging Chemoenzymatic and Radical-Based Retrosynthetic Logic for Rapid and Modular Synthesis of Oxidized Meroterpenoids. *Nat. Chem.* **2020**, *12*, 173-179.

(185) Zhang, X.; King-Smith, E.; Renata, H. Total Synthesis of Tambromycin by Combining Chemocatalytic and Biocatalytic C–H Functionalization. *Angew. Chem. Int. Ed.* **2018**, *57*, 5037-5041.

(186) Zwick, C. R.; Renata, H. A One-Pot Chemoenzymatic Synthesis of (2*S*, 4*R*)-4-Methylproline Enables the First Total Synthesis of Antiviral Lipopeptide Cavinafungin B. *Tetrahedron* **2018**, *74*, 6469-6473.

(187) Zwick, C. R.; Renata, H. Remote C–H Hydroxylation by an α -Ketoglutarate-Dependent Dioxygenase Enables Efficient Chemoenzymatic Synthesis of Manzacidin C and Proline Analogs. *J. Am. Chem. Soc.* **2018**, *140*, 1165-1169.

(188) Zhang, X.; Renata, H. Efficient chemoenzymatic synthesis of (2*S*,3*R*)-3-hydroxy-3-methylproline, a key fragment in polyoxypeptin A and FR225659. *Tetrahedron* **2019**, *75*, 3253-3257.

(189) Hayashi, T.; Ligibel, M.; Sager, E.; Voss, M.; Hunziker, J.; Schroer, K.; Snajdrova, R.; Buller, R. Evolved Aliphatic Halogenases Enable Regiocomplementary C–H Functionalization of a Pharmaceutically Relevant Compound. *Angew. Chem. Int. Ed.* **2019**, *58*, 18535-18539.

(190) Zwick, C. R.; Sosa, M. B.; Renata, H. Characterization of a Citrulline 4-Hydroxylase from Nonribosomal Peptide GE81112 Biosynthesis and Engineering of Its Substrate Specificity for the Chemoenzymatic Synthesis of Enduracididine. *Angew. Chem. Int. Ed.* **2019**, *58*, 18854-18858.

(191) Doyon, T. J.; Perkins, J. C.; Baker Dockrey, S. A.; Romero, E. O.; Skinner, K. C.; Zimmerman, P. M.; Narayan, A. R. H. Chemoenzymatic *o*-Quinone Methide Formation. *J. Am. Chem. Soc.* **2019**, *141*, 20269-20277.

(192) Duewel, S.; Schmermund, L.; Faber, T.; Harms, K.; Srinivasan, V.; Meggers, E.; Hoebenreich, S. Directed Evolution of an Fe^{II}-Dependent Halogenase for Asymmetric C(*sp*³)–H Chlorination. *ACS Catal.* **2020**, *10*, 1272-1277.

(193) Zhang, X.; King-Smith, E.; Dong, L.-B.; Yang, L.-C.; Rudolf, J. D.; Shen, B.; Renata, H. Divergent Synthesis of Complex Diterpenes Through a Hybrid Oxidative Approach. *Science* **2020**, *369*, 799-806.

(194) Mailyan, A. K.; Chen, J. L.; Li, W.; Keller, A. A.; Sternisha, S. M.; Miller, B. G.; Zakarian, A. Short Total Synthesis of [¹⁵N₅]-Cylindrospermopsins from ¹⁵NH₄Cl Enables Precise Quantification of Freshwater Cyanobacterial Contamination. *J. Am. Chem. Soc.* **2018**, *140*, 6027-6032.

(195) Baker Dockrey, S. A.; Lukowski, A. L.; Becker, M. R.; Narayan, A. R. H. Biocatalytic Site- and Enantioselective Oxidative Dearomatization of Phenols. *Nat. Chem.* **2018**, *10*, 119-125.

(196) Wang, Z. J.; Renata, H.; Peck, N. E.; Farwell, C. C.; Coelho, P. S.; Arnold, F. H. Improved Cyclopropanation Activity of Histidine-Ligated Cytochrome P450 Enables the Enantioselective Formal Synthesis of Levomilnacipran. *Angew. Chem. Int. Ed.* **2014**, *53*, 6810-6813.

(197) Hernandez, K. E.; Renata, H.; Lewis, R. D.; Kan, S. B. J.; Zhang, C.; Forte, J.; Rozzell, D.; McIntosh, J. A.; Arnold, F. H. Highly Stereoselective Biocatalytic Synthesis of Key Cyclopropane Intermediate to Ticagrelor. *ACS Catal.* **2016**, *6*, 7810-7813.

(198) Bajaj, P.; Sreenilayam, G.; Tyagi, V.; Fasan, R. Gram-Scale Synthesis of Chiral Cyclopropane-Containing Drugs and Drug Precursors with Engineered Myoglobin Catalysts Featuring Complementary Stereoselectivity. *Angew. Chem. Int. Ed.* **2016**, *55*, 16110-16114.

(199) Truppo, M. D. Biocatalysis in the Pharmaceutical Industry: The Need for Speed. *ACS Med. Chem. Lett.* **2017**, *8*, 476-480.

(200) Sheldon, R. A.; Woodley, J. M. Role of Biocatalysis in Sustainable Chemistry. *Chem. Rev.* **2018**, *118*, 801-838.

(201) Hauer, B. Embracing Nature's Catalysts: A Viewpoint on the Future of Biocatalysis. *ACS Catal.* **2020**, *10*, 8418-8427.

(202) Wu, S.; Snajdrova, R.; Moore, J. C.; Baldenius, K.; Bornscheuer, U. Biocatalysis: Enzymatic Synthesis for Industrial Applications. *Angew. Chem. Int. Ed.* **2020**, *59*, 2-34.

TOC Graphic:

